

Determination of Structures and Energetics of Small- and Medium-Sized One-Carbon-Bridged Twisted Amides using ab Initio Molecular Orbital Methods: Implications for Amidic Resonance along the C–N Rotational Pathway

Roman Szostak,[†] Jeffrey Aubé,[‡] and Michal Szostak^{*,§}

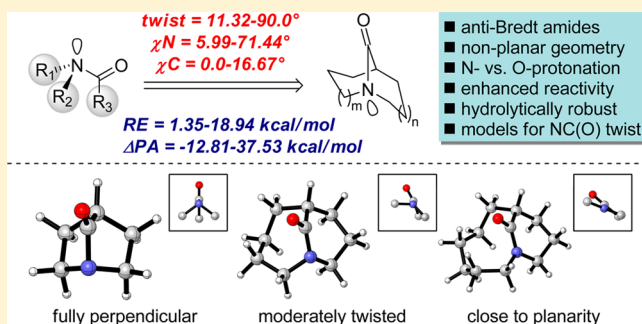
[†]Department of Chemistry, Wroclaw University, F. Joliot-Curie 14, Wroclaw 50-383, Poland

[‡]Division of Chemical Biology and Medicinal Chemistry, UNC Eshelman School of Pharmacy, University of North Carolina at Chapel Hill, Chapel Hill, North Carolina 27599, United States

[§]Department of Chemistry, Rutgers University, 73 Warren Street, Newark, New Jersey 07102, United States

S Supporting Information

ABSTRACT: Twisted amides containing nitrogen at the bridgehead position are attractive practical prototypes for the investigation of the electronic and structural properties of nonplanar amide linkages. Changes that occur during rotation around the N–C(O) axis in one-carbon-bridged twisted amides have been studied using ab initio molecular orbital methods. Calculations at the MP2/6-311++G(d,p) level performed on a set of one-carbon-bridged lactams, including 20 distinct scaffolds ranging from [2.2.1] to [6.3.1] ring systems, with the C=O bond on the shortest bridge indicate significant variations in structures, resonance energies, proton affinities, core ionization energies, frontier molecular orbitals, atomic charges, and infrared frequencies that reflect structural changes corresponding to the extent of resonance stabilization during rotation along the N–C(O) axis. The results are discussed in the context of resonance theory and activation of amides toward N-protonation (N-activation) by distortion. This study demonstrates that one-carbon-bridged lactams—a class of readily available, hydrolytically robust twisted amides—are ideally suited to span the whole spectrum of the amide bond distortion energy surface. Notably, this study provides a blueprint for the rational design and application of nonplanar amides in organic synthesis. The presented findings strongly support the classical amide bond resonance model in predicting the properties of nonplanar amides.



■ INTRODUCTION¹

The amide bond is one of the most important functional groups in chemistry and biology.^{1,2} The properties of amide linkages have been extensively studied from both theoretical³ and experimental perspectives.⁴ The $n_N \rightarrow \pi^*_{C=O}$ conjugation and the resulting planarity control the vast majority of the physicochemical properties of amides (Figure 1A), including (1) high barriers to cis–trans rotation of approximately 15–20 kcal/mol,⁵ (2) coplanarity of the six atoms comprising the amide bond,⁶ (3) short N–C(O) bonds (e.g., formamide, 1.349 Å),⁷ (4) long C=O bonds (e.g., formamide, 1.193 Å),⁷ (5) thermodynamically favored protonation at oxygen by approximately 10–15 kcal/mol,⁸ and (6) high resistance toward nucleophilic addition and hydrolysis (e.g., $t_{1/2}$ for neutral hydrolysis of Ac-Gly-Gly of approximately 500 years).⁹

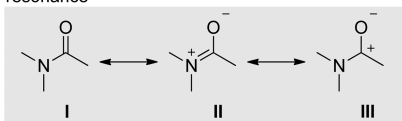
In contrast to planar amides, relatively little is known about the properties of distorted amides¹⁰ despite their profound implications for structure¹¹ and reactivity¹² and, most importantly, their far-reaching significance in biology and

medicinal chemistry (e.g., amide bond proteolysis,^{13a–c} isomerization of cis–trans peptides,^{13d–f} protein splicing,^{13g–j} enhanced activity of strained β -lactam antibiotics,^{13k,l} modulation of conformational preferences of peptides and proteins,^{13m–o} new lead structures in chemical space^{13p–s}). More fundamentally, examination of the reactivity of nonplanar amides that are characterized by ground-state distortion to systematically evaluate the effect of structural changes that occur during the amide bond rotation provides crucial insight into the amide bond resonance.^{1,2} Thorough predictions question the classic resonance model with the polarized canonical structure (III in Figure 1A; polarization model) proposed to account for the hindered cis–trans isomerization in amides.¹⁴ This model provides an explanation for the changes in bond lengths (the C–N bond lengthens approximately 8 times more than the C=O bond shortens)

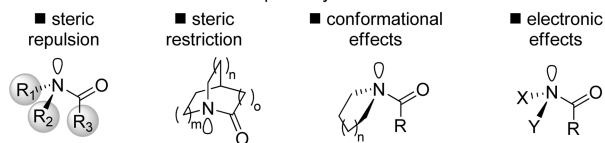
Received: April 20, 2015

Published: July 8, 2015

A. Amide bond resonance



B. General methods to achieve non-planarity of amide bonds



C. Restricting conformation of non-planar amides as bridged lactams

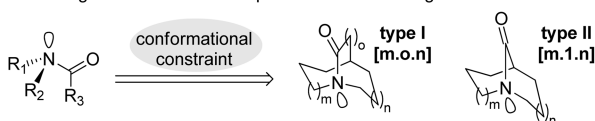


Figure 1. (a) Resonance description of amide bonds. (b) Geometric transformations resulting in nonplanarity of amides. (c) Conformational restriction of amides as bicyclic bridgehead lactams.

and charge densities (less variation in electron density at O than N) during the amide bond rotation;^{14d} however, the validity of the polarization model is a question of ongoing debate.^{1–4,14}

Several methods have been used to force geometrical transformations of amide bonds (Figure 1B).¹⁰ The most general synthetic approach involves steric restriction by constraining the amide bond in a bicyclic ring system in which the nitrogen atom is placed at a bridgehead position (Figures 1C and 2; bridged lactams, twisted lactams).^{10a–c}

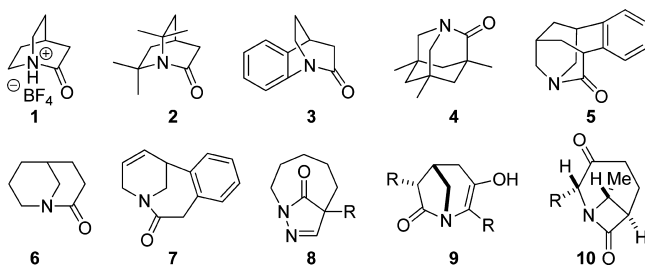


Figure 2. Selected examples of nonplanar bridged lactams reported previously.

Bridged lactams are classified as amides in which the N–C(O) bond is placed on a one-carbon bridge (type [m.1.n]) or a larger bridge (type [m.n.o]) (Figure 1C and Table 1).¹⁰ To date, extensive studies have focused on lactams in which the N–C(O) bond is placed on a bridge that is larger than one carbon.^{15–26} In particular, 2-quinuclidone derivatives with the first recognition of the analogy to anti-Bredt olefins by Lukeš in 1938,¹⁵ synthetic studies by Woodward,¹⁶ Yakhontov,¹⁷ and Pracejus,¹⁸ and the landmark 2006 synthesis of the parent 2-quinuclidonium tetrafluoroborate by Stoltz¹⁹ occupy a unique place in advancing our knowledge of the hyper-reactivity of nonplanar amides and their tendency to undergo rapid hydrolysis.^{13a–c} The synthesis of 2-quinuclidone derivatives by Brown²⁰ and Shea²¹ as well as the design and preparation of the essentially perpendicular 1-aza-2-adamantanone by Kirby²² and its extended analogues by Coe²³ are other noteworthy advances in the field. In recent years, several theoretical studies of bicyclic bridged lactams in which the N–C(O) bond is placed on a larger bridge have been reported.^{24–26} Most

importantly, Greenberg and co-workers determined the electronic and structural properties of bridgehead bicyclic lactams and demonstrated the hyperstability of larger lactams in the series.²⁴ Other studies have addressed the enhanced hydrolysis of twisted amides.²⁵ Theoretical investigations of the stability of the highly constrained 1-aza-2-adamantanone (Kirby's amide) have been reported.²⁶

Despite these remarkable theoretical advances, bridged lactams in which the N–C(O) bond is placed on a larger bridge have had limited practical applications for several reasons:²⁷ (i) The scope of the synthesis and the ease of scaffold modification and diversification are severely limited because of the lack of reliable synthetic protocols. (ii) Lactams from this class are often hydrolytically unstable, which necessitates excessive steric hindrance around the amide bond to enable their preparation and handling. These synthetic modifications negatively impact other reactive properties of the amide linkage. (iii) *Most importantly, because of the relative flexibility of ring systems containing amide bonds, these lactams do not span the whole spectrum of amide bond distortion and thus do not serve as good models for a comprehensive examination of the effect of geometry on the structures and energetics of nonplanar amides.*

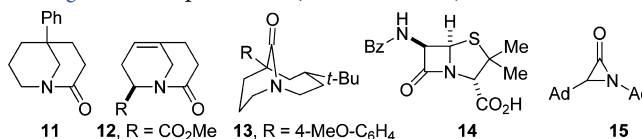
In contrast, bridged lactams in which the N–C(O) bond is located on a one-carbon bridge (one-carbon-bridged lactams) have recently received considerable attention as highly promising models to test the effect of amide bond distortion (Figure 1C and Table 1).^{10a,b} In 2007, Aubé and co-workers reported the classic synthesis of one-carbon-bridged lactams²⁸ employing electronically-controlled²⁹ intramolecular Schmidt rearrangement³⁰ of 2-azidoalkyl ketones by means of electrostatic cation– π interactions to direct the regiochemistry of the migrating bond. Efficient methods for the synthesis of other one-carbon-bridged twisted amides have been reported,³¹ providing robust protocols for the synthesis of a diverse array of compounds with a systematically varying distortion range (Winkler–Dunitz parameters; vide infra).³² Seminal studies on the reactivity of one-carbon-bridged amides demonstrated that these amides participate in a striking cleavage of unactivated σ C–N bonds adjacent to the nonplanar amide bond under mild hydrolysis conditions.³³ This transformation is initiated by activation of amide bonds by N-protonation. Furthermore, the first examples of isolated N-protonated one-carbon-bridged lactams featuring easily accessible medium-sized rings (cf. fully perpendicular 2-quinuclidone or 1-aza-2-adamantanone derivatives)^{12,19,22} have been reported and structurally characterized, including the first direct comparison of N-protonated amides with the parent neutral precursors.³⁴ Importantly, one-carbon-bridged lactams are hydrolytically robust because transannular scaffolding effects of medium-sized rings stabilize the closed lactam conformation (cf. the open amino acid form),³⁵ thus strongly suggesting that generic lactams characterized by a considerable distortion of amide bonds can be evaluated under standard laboratory conditions, which stands in sharp contrast to other classes of nonplanar amides.^{10,36}

Despite the aforementioned developments, a theoretical investigation of one-carbon-bridged lactams using a high level of theory has not been reported to date.^{3,14,24,37} This hampers further advances in the rational application of hydrolytically robust twisted amides, including as practical models to elucidate the structural and energetic changes that follow rotation around the N–C(O) bond during cis–trans isomerization of amides.^{13d–f}

Table 1. Summary of Structural Parameters of Representative Planar and Bridged Amides

entry ^a	amide	N–C(O) [Å]	C=O [Å]	τ [deg]	χ_N [deg]	χ_C [deg]
1 ^b	1	1.526	1.192	89.1	59.5	0.2
2 ^c	4	1.473	1.196	85.8	61.7	5.5
3 ^d	10	1.414	1.200	35.3	57.1	6.0
4 ^e	11	1.374	1.201	20.8	48.8	5.9
5 ^f	12	1.399	1.215	16.7	54.9	1.6
6 ^g	13	1.367	1.227	42.8	34.1	16.5
7 ^h	14	1.384	1.212	16.6	49.8	4.5
8 ⁱ	15	1.328	1.199	23.9	54.9	7.0
9 ^j	<i>N</i> -methylvalerolactam	1.329	1.242	2.8	2.6	1.7
10 ^k	formamide	1.349	1.193	0.0	0.0	0.0

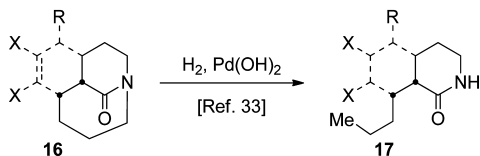
^aEntries 1–9 present X-ray data. Entry 10 shows calculated values. ^bReference 29. ^cReference 22a. The C=O group is disordered over two sites. Mean values of bond lengths and dihedral angles are shown. ^dReference 31f. ^eReference 27b. ^fReference 21. ^gReference 34a. ^hReference 27e. ⁱReference 27f, bond lengths (X-ray); ref 27g, distortion parameters (calculated values). ^jReference 27h. ^kReference 24.



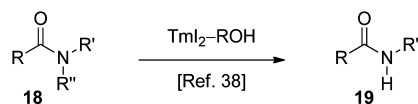
Herein we report a computational study to gain insight into the structures and energetic parameters of one-carbon-bridged twisted lactams. The presented results provide new insights into the fundamental question of amidic resonance upon amide bond rotation^{1–4} and should enable further developments in the design of new generic modes of reactivity of nonplanar amides.^{10a} The current study was stimulated by the advances in the area of one-carbon-bridged twisted lactams (vide supra)^{28,33–35} as well as by the recent discovery that thulium(II) iodide (TmI₂), a single-electron-transfer lanthanide(II) reagent, promotes the cleavage of unactivated σ C–N bonds adjacent to amide bonds in simple amides,³⁸ a process that is formally analogous to the previously observed C–N bond scission in one-carbon-bridged amides via hydrogenolysis (Scheme 1).³³ The aim of the current study was to

Scheme 1. Cleavage of Activated and Unactivated σ C–N Bonds in Amides

A. σ C–N bond cleavage in non-planar amides



B. TmI₂-promoted σ C–N bond cleavage in planar amides



determine the distortion and energetics of small- and medium-sized one-carbon-bridged lactams, with the major focus on understanding the changes that occur during rotation around the N–C(O) axis and their effect on the pyramidalization at nitrogen.²⁴ We hypothesized that mapping the amide bond distortion along energetic parameters of amide bonds over a sufficiently large distortion range should enable elucidation of the role of strain and the overlap of the nitrogen lone pair and the carbonyl π system on the reactivity of nonplanar amides. From the outset, we recognized that if a correlation between structure and energetics could be realized, then the study would

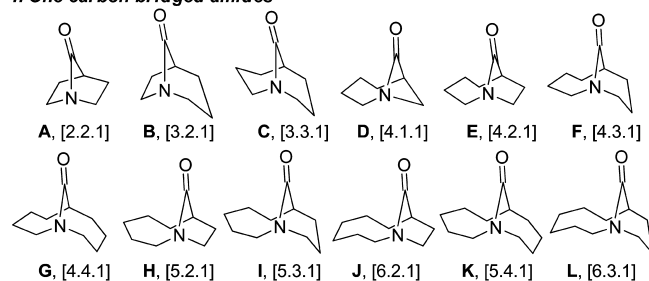
shed light on the amide bond resonance model using nonplanar amides that have already been synthesized in a laboratory environment (cf. theoretical investigation) and validated experimentally.

The data described in this article show the following important features: (1) There is a direct correlation between structures and energetics in nonplanar distorted amides with gradually varying distortion that spans the whole spectrum of distortion range: $\tau = 11.32$ – 90.0° ; $\chi_N = 5.99$ – 71.44° ; $\chi_C = 0.0$ – 16.67° .³² (2) Energetic parameters explain the chemical reactivity of one-carbon-bridged twisted lactams, including the C–N bond cleavage, acyl substitution reactions, and hydrolytic stability observed experimentally in previous studies.^{33–35} (3) One-carbon-bridged twisted amides span a diverse range of distortion and electronic parameters, which demonstrates that these compounds may serve as formal “amino-ketone” equivalents with tunable $n_N \rightarrow \pi^*_{C=O}$ donation.^{8,10,12} (4) Examination of amides that cover the whole span of distortion range sheds new light on the amidic resonance, including an answer to the long-standing question of what structural factors govern the N- versus O-protonation switch in nonplanar amides.²⁴ (5) The structural and energetic changes that occur during the amide bond rotation in these model systems strongly support the classical amide resonance model.^{1–4,14,24}

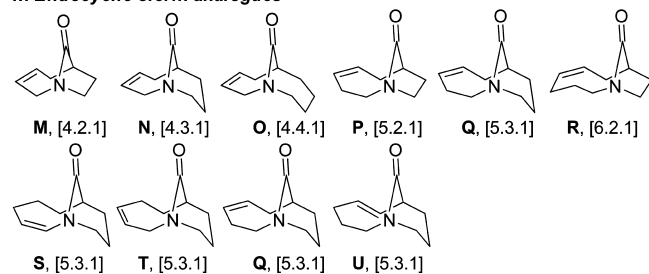
RESULTS AND DISCUSSION

The conceptual advantage of using one-carbon-bridged twisted amides (cf. analogues with two-carbon or larger bridges)¹⁰ is evident from their stability toward hydrolysis,³⁵ their successful use as a platform for the discovery of new reactivity of amide bonds,^{33,34} and the accessibility of diverse ring systems.³¹ Figure 3 depicts one-carbon-bridged amides selected for the present study. These compounds were selected on the basis of their synthetic accessibility and distortion range of amide bonds. Amides in which the overall sum of carbon atoms forming the core 1-azabicyclo scaffold is less than five were excluded from the study because these compounds are too strained to exist. Conversely, amides in which the sum of carbon atoms is more than ten feature more flexible ring systems with properties analogous to those of planar amides. These compounds are outside the scope of the current

I. One-carbon-bridged amides



II. Endocyclic olefin analogues



III. Tricyclic and bicyclic [4.3.1] analogues

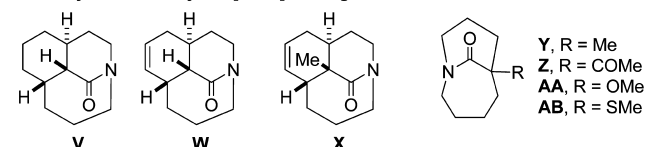


Figure 3. Structures of small- and medium-sized one-carbon-bridged lactams calculated in the current study.

investigation. Three general classes of compounds were selected for the study: parent scaffolds (Figure 3A), olefin-containing analogues (Figure 3B), and substituted analogues of the [4.3.1] system, which has been the most studied ring system of bridged amides to date (Figure 3C).

Bridged lactams containing the selected parent scaffolds (Figure 3A) have been previously reported,^{28,31,33} although the amides containing the first two rings in the series may be too strained to be isolated. (i) A bridged amide containing the [2.2.1] ring system has been proposed as an intermediate in the biomimetic synthesis of communsins.^{31g} (ii) Bridged lactams containing the [3.2.1] amide ring system were prepared (but not isolated) by Murphy^{31d} and Nazarenko^{31h} via the intramolecular Schmidt reaction and the intramolecular amide–imine condensation, respectively. (iii) The [3.3.1] amide ring system was synthesized via transannular amidation.^{31a} This ring system was predicted to contain a perpendicular amide bond on the basis of its reactive and spectroscopic properties.^{31e} (iv) The [4.1.1] amide ring system was synthesized by Williams^{31f} via Rh-catalyzed carbene insertion into the NH bond. This is the only example in the selected series featuring an azetidine ring; the properties of these lactams are influenced by the inherent strain of the β -lactam ring despite their bridged structures.^{13k,l} (v) Amides containing [4.2.1], [4.3.1], and [5.3.1] ring systems are readily available via the intramolecular Schmidt reaction using cation– π ^{28,31c} and cation– n ^{31b} regiochemistry-controlling elements. (vi) Amides containing [4.2.1], [4.3.1], [4.4.1], [5.2.1], [5.3.1], and [6.2.1] ring systems have been synthesized via transannular amidation.^{31a} Several of these scaffolds were prepared by Schill and co-workers during the synthesis of vinca alkaloids.^{31i–k} (vii) Amides containing [5.4.1] and [6.3.1] ring systems were

synthesized by Schill^{31k} and Ban^{31l} via transannular amidation and intramolecular alkylation, respectively. (viii) The syntheses of several larger ring systems have been reported.^{31m–o} On the basis of the reactive properties and available X-ray crystallographic studies^{10a} (vide infra), we hypothesized that the selected series of 12 lactams would be characterized by a gradually decreasing distortion of the amide bond and thus would offer a systematic approach for probing the effect of structure on the properties of distorted amide linkages.

Amides featuring endocyclic olefins were selected as the second class of compounds for the study (Figure 3B). On the basis of the experimental reactive properties,^{31a,33,34a} we hypothesized that this simple modification would provide amides with structural and energetic parameters that do not overlap in the distortion space with unconstrained lactams. Moreover, systematic determination of geometries and energetics would provide insight into the C–N hydrogenolysis reaction of nonplanar amides;^{31a,33} experimentally, it has been shown that the reactivity of amides bearing internal olefins toward C–N hydrogenolysis decreases in the order [4.3.1] ring system (3:1 cleavage selectivity) > [4.4.1] ring system (1:1 cleavage selectivity) > [4.2.1] ring system (cleavage not observed)^{31a} and is lower than that of tricyclic bridged amides bearing the [4.3.1] ring system (vide infra).³³ The effect of migrating the endocyclic olefin within a larger ring was tested using a representative [5.3.1] ring system. This variation was introduced to probe the effect of additional rigidity on the properties of amide bonds. The amide scaffolds presented in Figure 3B have been synthesized via ring-closing metathesis/transannular amidation, including a one-pot procedure.^{31a}

Substituted analogues of the [4.3.1] ring system were selected as the third class of compounds (Figure 3C). To date, one-carbon-bridged twisted amides containing the [4.3.1] ring system have been the most comprehensively studied in the literature.^{10a} We hypothesized that detailed information about structures and energetics would provide insights into the factors governing their experimentally observed reactivities and facilitate the rational design of novel analogues. Specifically, we sought to probe the structural and energetic differences determining the C–N bond cleavage reactivities as well as the enhanced stability of some of these amides as determined experimentally.^{31a,33,34a} Experiments have shown that tricyclic bridged lactams containing [4.3.1] ring systems are more reactive than the corresponding bicyclic bridged lactams,^{33,34a} and the presence of an additional α -substituent enhances the hydrolytic stability in the series.³⁵ Amides for this study were selected on the basis of their synthetic availability,^{28,31,33–35} supported by the experimental reactivity studies,^{31a,33–35} and include the following compounds: (i) tricyclic amides prepared via domino Diels–Alder/Schmidt reactions,²⁸ (ii) bicyclic lactams containing α -heteroatom substituents synthesized via cation– n -controlled Schmidt reactions,^{31b} (iii) bicyclic lactams containing an α -methyl substituent prepared via 1,3-diaxial-interaction-controlled Schmidt reactions,²⁸ and (iv) bicyclic lactams containing α -carbonyl groups synthesized via transannular amidation.^{31a} α -Functionalized bicyclic analogues have been previously described,^{31c} these compounds are also accessible via bridgehead deprotonation/alkylation, as reported by Hayes and Simpkins.³⁹ Additionally, a tricyclic saturated bridged lactam was selected for the study because previous work has shown that modifications of the distal olefin in the tricyclic [4.3.1] ring system result in significant changes in the

Table 2. Total Energies and Selected Geometric Parameters for Optimized Structures of Bridged Amides Calculated at the MP2/6-311++G(d,p) Level^a

entry	amide	$-E_T$ [au]	$-E_T$ (corr) [au]	N–C(O) [Å]	C=O [Å]	τ [deg]	χ_N [deg]	χ_C [deg]
1	A	363.06051	362.90686	1.474	1.201	90.00	71.44	0.00
2	B	402.27281	402.08837	1.447	1.209	65.40	63.10	7.66
3	C	441.46867	441.25388	1.446	1.212	90.00	53.20	0.00
4	D	402.25553	402.07156	1.422	1.207	38.23	57.48	6.33
5	E	441.47896	441.26376	1.401	1.218	36.90	47.69	11.17
6	F	480.67239	480.42708	1.391	1.225	41.78	36.01	15.42
7	G	519.86734	519.59194	1.409	1.223	47.52	41.78	11.53
8	H	480.68637	480.44070	1.381	1.223	21.97	32.11	7.62
9	I	519.87533	519.59957	1.372	1.230	25.53	17.39	10.67
10	J	519.88300	519.60699	1.365	1.228	11.32	5.99	4.94
11	K	559.05973	558.75395	1.378	1.231	37.94	14.10	13.87
12	L	559.07658	558.77041	1.367	1.233	18.84	12.19	7.97
13	M	440.26254	440.07230	1.406	1.216	33.49	52.09	9.47
14	N	479.45319	479.23261	1.401	1.222	43.15	46.71	13.10
15	O	518.64480	518.39414	1.409	1.222	46.21	44.37	11.42
16	P	479.45540	479.23436	1.384	1.221	19.44	37.02	7.60
17	Q	518.66161	518.41086	1.392	1.223	34.53	28.55	9.04
18	R	518.65817	518.40698	1.370	1.226	22.39	20.60	9.17
19	S	518.65131	518.40072	1.386	1.224	30.34	23.29	10.15
20	T	518.65687	518.40558	1.380	1.228	27.33	30.52	10.35
21	U	518.65511	518.40388	1.375	1.228	24.59	27.03	9.10
22	V	597.06436	596.75198	1.415	1.219	58.20	45.09	11.54
23	W	595.85508	595.56744	1.415	1.220	56.95	44.08	11.56
24	X	635.05765	634.74062	1.409	1.222	54.93	41.33	11.92
25	Y	519.87486	519.60044	1.388	1.226	41.93	33.76	15.67
26	Z	632.95910	632.67347	1.384	1.227	41.01	35.53	15.99
27	AA	594.92748	594.64720	1.384	1.226	42.84	30.26	17.53
28	AB	917.53720	917.25992	1.386	1.225	42.93	31.55	16.67

^aFor X-ray data on the 2-(*tert*-butoxycarbonyl)-3-keto-8-methyl derivative of **D**, see ref 31f. For X-ray data on the 3-*tert*-butyl-6-(4-methoxyphenyl) derivative of **E**, see ref 34a (also see Table 1). For X-ray data on benzo-fused derivatives of 2-quinuclidone, see ref 20a. For computational data (6-31G*) on 2-quinuclidone derivatives, see ref 24a,b. For X-ray data on bicyclo[*n*.3.1] (*n* = 3–5) bridgehead lactams/olefins, see ref 21. See Figure 3 for structures **A**–**AB**.

amide bond distortion (e.g., τ changes from 51.5° to 72.4° upon hydroxylation of the olefin).^{10a}

Ab initio molecular orbital calculations were carried out at the MP2/6-311++G(d,p) level. This method has been shown to be accurate in predicting properties and resonance energies of amides^{3h,24a} (e.g., for the resonance energy of *N,N*-dimethylacetamide, the experimental and calculated values are 16.8 ± 1.3 and 16.4 kcal/mol, respectively). This method was further verified by obtaining good correlations between the calculated structures and available X-ray structures in the series; the parent [4.3.1] bridged bicyclic lactam (τ = 41.78°; χ_N = 36.01°; χ_C = 15.42°) versus the X-ray structure of an α -4-methoxyphenyl derivative (τ = 42.8°; χ_N = 34.1°; χ_C = 16.5°),^{34a} which is one of the few available twisted amide geometries that has been determined in the solid state.^{10a} Several X-ray structures of one-carbon-bridged lactams have been reported;^{10a} however, these structures are exclusively limited to derivatives of the [4.3.1] ring system^{28,34a} and one X-ray structure of the [4.1.1] ring system (τ = 35.3°; χ_N = 57.1°; χ_C = 6.0°),^{31f} for which a very accurate calculated structure at the MP2/6-311++G(d,p) level has also been found (parent lactam: τ = 38.23°; χ_N = 57.48°; χ_C = 6.33°). Because of the conformational constraint of bridged systems, calculations of energy minima of unsubstituted medium-bridged bicyclic lactams typically result in a significant reduction of computational time compared with similar molecules with large degrees

of conformational freedom.²⁴ The use of lower-level methods to compute the properties of amides has been shown to be problematic because of inaccuracies in the treatment of *N*-inversion barriers.^{3a,h,24,37} To the best of our knowledge, the optimization of structures of nonplanar amides using a high level of theory has not been reported to date. Computational methods and Cartesian coordinates and energies for all of the reported structures are given in the Supporting Information (SI).⁴⁰

Structures and Total Energies. Total energies of one-carbon-bridged twisted lactams together with values including zero-point energy and thermal corrections as well as selected structural parameters are listed in Table 2. Optimized geometries of the major lactam ring systems (Figure 3A) as well as Newman projections along the N–C(O) axis are presented in Figure 4. Optimized geometries of the more advanced ring systems (Figure 3B,C) and Cartesian coordinates with energies for all of the computed structures are presented in the SI (Figure SI-1). Optimized total energies for all of the species calculated in the current study (bridged amides, amines, ketones, and hydrocarbons) are presented in the SI (Table SI-1). In this section, the discussion focuses on the properties of the major ring systems (Figure 3A), followed by correlations using the more advanced scaffolds (Figure 3B,C).

Geometries of One-Carbon-Bridged Lactams. The results in Table 2 validate the use of small- and medium-sized one-

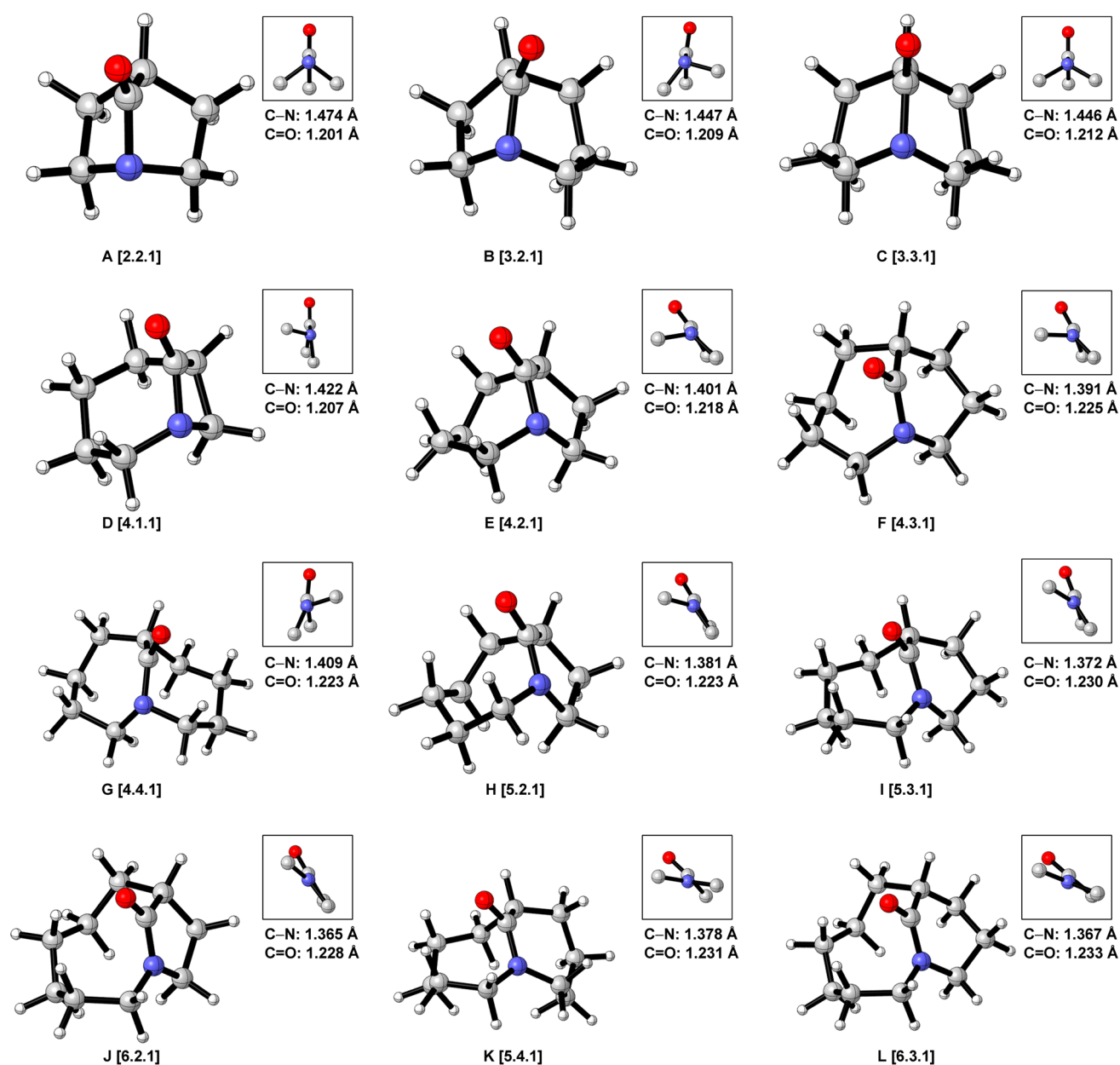


Figure 4. Optimized geometries of bridged lactams A–L (MP2/6-311++G(d,p)). The insets show Newman projections along the N–C(O) axis. For clarity, the Newman projections are presented in the same orientation as the lactam geometries. Bond lengths are given in Å. For optimized geometries of bridged lactams M–AB (MP2/6-311++G(d,p)), see the SI. See Figure 3 for structures A–L.

carbon-bridged twisted amides^{28,31,33–35} as models for a systematic study of geometric changes that occur during amide bond rotation.^{1–4} The selected set of bridged amide homologues covers the whole spectrum of amide bond distortion geometries.³² The twist angle changes from essentially planar to fully perpendicular ($\tau = 11.32$ – 90.0°), while the pyramidalization at nitrogen varies from essentially sp^2 -hybridized to fully sp^3 -hybridized nitrogen ($\chi_N = 5.99$ – 71.44°). In contrast, the pyramidalization at carbon remains relatively unchanged with the carbonyl carbon essentially planar in the series ($\chi_C = 0.0$ – 15.42°), which is consistent with the previous observations regarding amide bond distortion.^{10–12} In agreement with the amide bond distortion parameters, the length of the N–C(O) bond varies between 1.474 and 1.365 Å for the [2.2.1] and [6.2.1] ring systems, respectively, while the length of the C=O bond is between 1.201 Å for the [2.2.1]

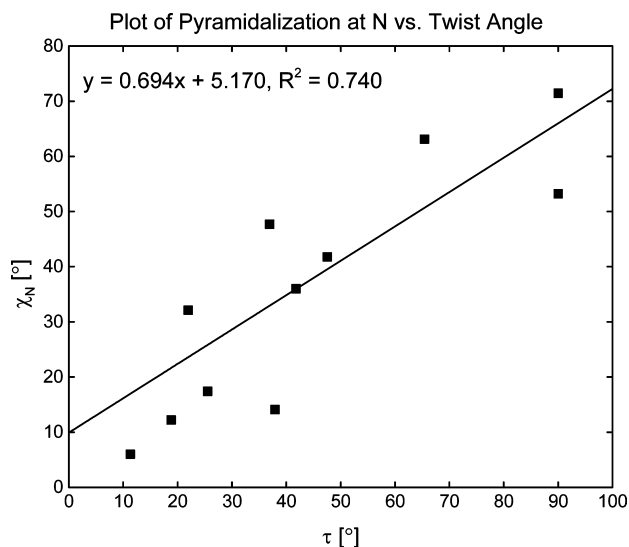
ring system and 1.233 Å for the [6.3.1] ring system (1.228 Å for the [6.2.1] ring system).

The most distorted amide in the series is compound A, [2.2.1]. This amide features the perfectly orthogonal amide bond and the pyramidal nitrogen atom ($\tau = 90.0^\circ$; $\chi_N = 71.44^\circ$). Interestingly, the least distorted compound in the series is amide J, [6.2.1] ($\tau = 11.32^\circ$; $\chi_N = 5.99^\circ$) rather than K, [5.4.1] ($\tau = 37.94^\circ$; $\chi_N = 14.10^\circ$) or L, [6.3.1] ($\tau = 18.84^\circ$; $\chi_N = 12.19^\circ$) despite their apparently more flexible ring systems.⁴¹ Thus, the data in Table 2 indicate that the use of five-membered rings to constrain the amide bond geometry is less efficient than the use of six- or even seven-membered rings (e.g., compare [4.3.1], [4.4.1], and [5.2.1] lactam scaffolds), which likely results from the inability of five-membered rings to adopt a pseudochair conformation in a strained bicyclic ring system. The role of transannular strain on the increased

distortion of bridged oxazinolactams^{42a-c} and 1,2-diazines^{42d} bearing larger ring systems has been noted. In the remaining compounds in Table 2, gradual changes in the amide bond distortion correlate well with the relative flexibilities of the ring systems (Table 2 and Figure 4). One amide that deserves a comment is lactam C, [3.3.1] ($\tau = 90.0^\circ$; $\chi_N = 53.20^\circ$). To our knowledge, this is only the third twisted lactam containing a perfectly orthogonal amide bond that has been synthesized and characterized experimentally to date^{31e} (the other two being 1-aza-2-adamantanone, 4^{22a} and 2-quinuclidonium tetrafluoroborate, 1¹⁹). The data in Table 2 suggest that this amide would be an interesting system for further reactivity studies.^{10a,33-35} In summary, the results in Table 2 show that the studied lactams can be divided into two categories based on the degree on distortion. A cutoff point for significantly distorted amides is located around the [4.4.1] ring system; however, even the less distorted scaffolds such as [5.2.1] to [6.3.1] contain decidedly nonplanar amide bonds (e.g., the second least distorted amide in the series, J, [6.2.1], suffers 21% of the maximum twist angle distortion, while its χ_N value corresponds to $sp^{2.20}$ hybridization, or approximately 20% of the loss of the $n_N \rightarrow \pi^*_{C=O}$ conjugation).

Interestingly, a plot of nitrogen pyramidalization versus twist angle gives a good correlation in the series (12 parent lactams, applying outlier analysis, lactam D, [4.1.1],^{31f} $Y = 0.69X + 5.17$, $R^2 = 0.74$), which indicates that the N–C(O) bond rotation is generally followed by changes in the pyramidalization at nitrogen; however, scattering characteristic of medium-sized ring scaffolding is also observed (Chart 1).^{10a,42} Thus, one-

Chart 1. Correlation of the Pyramidalization at Nitrogen (χ_N) with the Twist Angle (τ) for Amides A–L^a



^aLeave-one-out analysis: the outlier, with $\tau = 38.23^\circ$ and $\chi_N = 57.48^\circ$, represents compound D, [4.1.1] (azetidine). For an extended plot of χ_N versus τ , see the SI.

carbon-bridged lactams can be compared with anomeric amides,^{36a,b} which are characterized by changes in the pyramidalization at nitrogen, and with sterically distorted amides,^{10d,36c} featuring changes in the twist angles as the main geometric transformation of the amide bond (Figure 1B). Extended correlations involving other compounds in the study (Figure 3A–C) are presented in the SI. In general, good

agreement between the major and substituted ring systems was found; however, in some cases structural and energetic parameters are influenced by substitution, as expected.

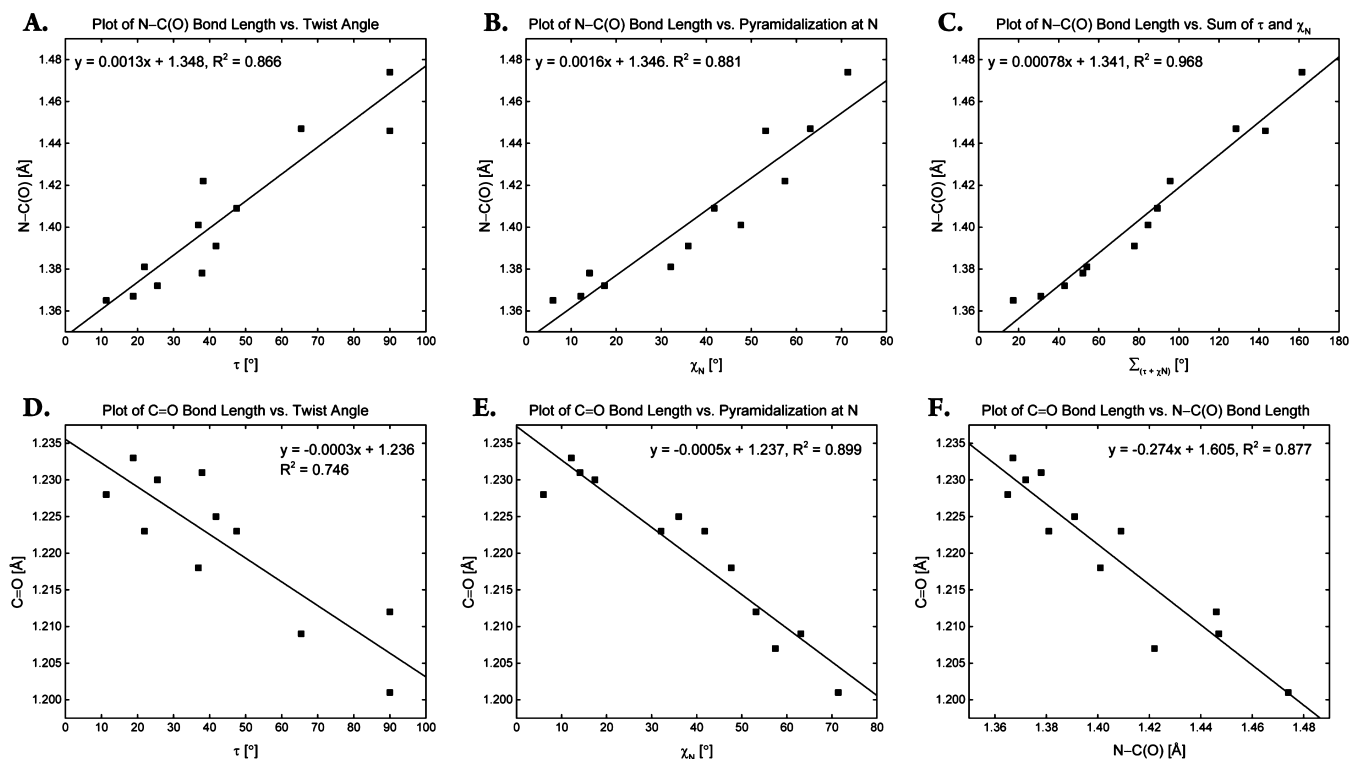
Relationship between Distortion and Amide Bond Geometry. A more detailed analysis of the structural data presented in Table 2 demonstrates the effect of amide bond distortion on its geometry, including changes in the bond lengths and relevant dihedral angles.²⁴ In agreement with the classical resonance model,^{1-4,14g} disruption of the $n_N \rightarrow \pi^*_{C=O}$ delocalization should result in a significant lengthening of the N–C(O) bond, while the C=O bond should experience relatively minor shortening. The effect of N–C(O) bond rotation on the geometric properties of amides has been the subject of numerous theoretical studies employing amides that are planar in the ground state.^{3a,b,5,14a} In contrast, few investigations have been reported that systematically address the relationship between distortion and geometric features of amides in readily accessible practical models that are nonplanar in the ground-state conformation.²⁴ The present study validates structural changes that occur with the N–C(O) bond rotation as a function of the twist angle and the pyramidalization at nitrogen. Several features are noteworthy (Figure 4, Chart 2).

For the N–C(O) bond, a plot of N–C(O) bond length versus twist angle gives a good linear correlation in the series (12 parent lactams, $Y = 0.0013X + 1.35$, $R^2 = 0.87$; Chart 2A). Moreover, a plot of N–C(O) bond length versus nitrogen pyramidalization gives a good linear correlation (12 parent lactams, $Y = 0.0016X + 1.35$, $R^2 = 0.88$; Chart 2B). Most importantly, a plot of N–C(O) bond length versus the sum of the twist angle and nitrogen pyramidalization, $\Sigma_{(\tau+\chi_N)}$ gives an excellent linear correlation over the observed range of amide bond geometries (12 parent lactams, $Y = 0.00078X + 1.34$, $R^2 = 0.97$; Chart 2C).

For the C=O bond, a plot of C=O bond length versus twist angle gives a relatively scattered negative linear relationship (12 parent lactams, applying outlier analysis, $Y = -0.00031X + 1.24$, $R^2 = 0.75$; Chart 2D). A plot of C=O bond length versus nitrogen pyramidalization gives a negative linear relationship (12 parent lactams, $Y = -0.00046X + 1.24$, $R^2 = 0.90$; Chart 2E). Finally, a plot of C=O bond length versus N–C(O) bond length gives a negative linear correlation in the series (12 parent lactams, $Y = -0.274X + 1.605$, $R^2 = 0.88$; Chart 2F).

There is also a linear correlation between the lengths of the C–N bonds adjacent to the amide bond and the sum of the twist angle and nitrogen pyramidalization, $\Sigma_{(\tau+\chi_N)}$, with a more accurate fit for the length of the C–N bond that is more distorted from planarity with the carbonyl group (12 parent lactams, $Y = -0.00023X + 1.45$, $R^2 = 0.80$; not shown). Correlations of the pyramidalization at carbon and the length of the C–C bond adjacent to the carbonyl group with other geometric parameters of the amide bond give scattered results.

Overall, these structural features indicate that an increase in the amide bond distortion results in a significant lengthening of the N–C(O) bond, while the C=O bond remains relatively unchanged in the studied family of nonplanar amides. This provides a strong support for the classical resonance model.^{1-4,14g} Interestingly, changes in the C=O bond length more closely follow variations in the pyramidalization at nitrogen than rotation around the N–C(O) axis. The pyramidalization at carbon and the length of the C–C bond adjacent to the amide bond are relatively insensitive to the

Chart 2. Correlations between Distortion and Geometric Features for Amides A–L^a

^aThe following correlations are shown: (A) Correlation of N–C(O) bond length with twist angle (τ). (B) Correlation of N–C(O) bond length with pyramidalization at nitrogen (χ_N). (C) Correlation of N–C(O) bond length with the sum of the twist angle and pyramidalization at nitrogen ($\Sigma(\tau + \chi_N)$). (D) Correlation of C=O bond length with twist angle (τ). Leave-one-out analysis: the outlier, with C=O bond length = 1.207 Å and $\tau = 38.23^\circ$, represents compound D, [4.1.1]. (E) Correlation of C=O bond length with pyramidalization at nitrogen (χ_N). Leave-one-out analysis: the outlier, with C=O bond length = 1.228 Å and $\chi_N = 5.99^\circ$, represents compound J, [6.2.1] ($Y = -0.001X + 1.240, R^2 = 0.945$; not shown). (F) Correlation of C=O bond length with N–C(O) bond length. For extended plots, see the SI.

changes in geometry upon rotation. Studies involving other classes of distorted amides are ongoing to verify the generality of the observed structural effects. In addition, solvent effects are known to influence the extent of amide bond resonance (e.g., by hydrogen bonding) and thus may modify the observed N–C(O) rotational effects.^{24b} The ability of nonplanar amides to access higher-energy intermediates (e.g., via conformational changes) should also be taken into account when predicting properties of nonplanar amides.^{12c}

A more detailed analysis reveals an interesting structural feature in that the N–C–O angles are smaller than the C–C–O angles, which is indicative of the early stage of the N–C(O) bond cleavage (three exceptions in the series are noted below).^{13a–c,24a,25} A comprehensive list of N–C–O and C–C–O angles as well as other geometric parameters is presented in the SI (Table SI-2). There appear to be a negative linear correlation between the C=O bond length and the difference in the C–C–O and N–C–O angles, $\Delta_{(\text{CCO}-\text{NCO})}$ (12 parent lactams, $Y = -0.0044X + 1.23, R^2 = 0.84$; not shown, see the SI) and a positive linear correlation between $\Delta_{(\text{CCO}-\text{NCO})}$ and the pyramidalization at nitrogen (outlier analysis, [6.2.1] scaffold, $Y = 0.101X - 2.25, R^2 = 0.80$; not shown, see the SI), providing further support for the initial stages of the amide bond cleavage. The average difference between the C–C–O and N–C–O angles is significantly larger than in the previously computed 1-azabicyclo[2.2.2]octan-2-one and 1-azabicyclo[3.3.1]nonan-2-one systems (12 parent amides, average of 1.85° vs 0.45°),^{24a} which appears to be characteristic

of twisted amides supported by the transannular effects of medium-sized rings.^{10a} In the following amides, the N–C–O angles are larger than C–C–O angles: (i) F, [4.3.1] ($\Delta_{(\text{CCO}-\text{NCO})} = -0.03^\circ$); (ii) K, [5.4.1] ($\Delta_{(\text{CCO}-\text{NCO})} = -0.80^\circ$); (iii) L, [6.3.1] ($\Delta_{(\text{CCO}-\text{NCO})} = -1.09^\circ$). In particular, the presence of amide F in this group is unexpected and suggests that the [4.3.1] scaffold exhibits higher stability due to conformational effects, which is consistent with the enhanced stability of the [4.3.1] ring system observed experimentally.^{33–35}

Advanced Ring Systems. Geometric parameters for one-carbon-bridged lactams containing olefins^{31a} and substituted [4.3.1] ring systems^{28,31b,c,33–35} (Figure 3B,C) are presented in Table 2 (entries 13–28). The data in Table 2 reveal that restriction of the conformational flexibility of one of the rings results in a significant increase in the amide bond distortion. A considerable increase is observed in larger ring systems such as Q, [5.3.1] and R, [6.2.1]; however, appreciable changes to the amide bond geometry are also present in more flexible lactams such as N, [4.3.1]. The data suggest higher reactivity of the amide bond in bridgehead lactams containing internal olefins, as observed experimentally.^{31a} Systematic positional migration of the double bond in a representative scaffold, [5.3.1], reveals that the internal double bond determines the degree of distortion, with the maximum observed for the most conformationally restricted ring system.⁴¹ Overall, these findings demonstrate that structural changes at positions distal from the amide bond can have a significant effect on its distortion. A

related increase in the amide bond distortion by the presence of distal substituents has been noted in the literature.⁴² Importantly, our results indicate that a judicious choice of ring substitution may result in a range of amide bond distortions within the same scaffold of bridgehead lactams. *This in turn can be exploited to fine-tune the reactivity^{10a} as well as drug–receptor interactions⁴³ from the experimental perspective.*

The data in Table 2 reveal structural changes in substituted [4.3.1] ring systems (Figure 3C). The computed structures of tricyclic bridged lactams containing the [4.3.1] scaffold (Table 2, entries 22–28) confirm that the amide bonds contained in these tricyclic ring systems are considerably more strained than the amide bonds contained in the corresponding bicyclic rings. This rigidifying effect is analogous to structural properties of bridged lactams containing endocyclic olefins (Figure 3B); in this case, however, restriction of the conformational flexibility results from the presence of an additional ring rather than an internal olefin. It should be noted that this conformational arrangement provides yet another method to increase the distortion of amide bonds. The data in Table 2 indicate that the presence of an α -substituent results in a decrease in amide bond distortion as manifested by changes in bond lengths and distortion parameters. While the effect is relatively small, it likely contributes to the lower stability of α -unsubstituted one-carbon-bridged twisted amides observed experimentally.³⁵ There are no significant changes to the amide bond geometry when electronically differentiated substituents are present at the α -position of the amide bond (vide infra, Protonation Sites and Proton Affinities). Overall, these findings highlight the importance of conformational constraints in achieving gradual levels of distortion of amide bonds *within the same ring system of bridged lactams* and provide significant insight into the experimental results observed previously.

Additive Twist Angle/Pyramidalization at Nitrogen Geometric Parameters. Analysis of the results presented in Table 2 demonstrates that description of the amide bond distortion by the sum of the twist angle and nitrogen pyramidalization, $\Sigma_{(\tau+\chi_N)}$ provides a more accurate representation of the geometric properties of nonplanar amides than the twist angle or the pyramidalization at nitrogen alone (Chart 1). Previous studies demonstrated that 1-azabicyclo[3.3.1]nonan-2-one (X-ray data for a phenyl analogue: $\tau = 20.8^\circ$; $\chi_N = 48.8^\circ$; $\chi_C = 5.9^\circ$; $\Sigma_{(\tau+\chi_N)} = 69.6^\circ$)^{27b,34b} and derivatives of one-carbon-bridged amides containing the [4.3.1] ring system (X-ray data for an aryl analogue: $\tau = 42.8^\circ$; $\chi_N = 34.1^\circ$; $\chi_C = 16.5^\circ$; $\Sigma_{(\tau+\chi_N)} = 76.9^\circ$)^{34a} feature amide bonds that are predominantly protonated at nitrogen. It was subsequently proposed that a twist angle of as low as 40–50° alone may be sufficient to promote N-protonation of amide bonds.^{34a,b} Additionally, earlier reports by Brown demonstrated that extended 2-quinuclidone analogues favor N-alkylation (X-ray data for the [3.2.2] amide ring system: $\tau = 33.2^\circ$; $\chi_N = 52.8^\circ$; $\chi_C = 11.0^\circ$; $\Sigma_{(\tau+\chi_N)} = 86.0^\circ$) or O-alkylation (X-ray data for the [3.3.2] ring system: $\tau = 15.3^\circ$; $\chi_N = 38.6^\circ$; $\chi_C = 4.3^\circ$; $\Sigma_{(\tau+\chi_N)} = 53.9^\circ$);⁴⁴ detailed experimental results were not disclosed. The additive parameter $\Sigma_{(\tau+\chi_N)}$ normalizes these results and reveals that a $\Sigma_{(\tau+\chi_N)}$ value of 60–70° appears to be close to a barrier between N- and O-protonation of amides. It should be noted that this value is much lower than the distortion that would correspond to a fully perpendicular amide bond ($\Sigma_{(\tau+\chi_N)} = 150.0^\circ$), which

has been proposed to be required for N-protonation.^{10,19,22} Given the availability of distorted amides in the moderate distortion range,^{10a,11} our data suggest that a wide range of amide analogues can be readily applied to probe the unconventional reactivity of amide bonds via N-protonation.⁴⁵ In the case of one-carbon-bridged lactams, the data in Table 2 suggest that one-carbon-bridged twisted amides ranging from A, [2.2.1] to G, [4.4.1] should predominantly undergo protonation/alkylation at nitrogen, while other amides in this series (H, [5.2.1] to L, [6.3.1]) may require more forcing conditions and/or further destabilization of the ground-state geometry to effect protonation/alkylation at the nitrogen atom (vide infra Protonation Sites and Proton Affinities for verification of this analysis).

Resonance Energies. A large barrier to rotation around the N–C(O) bond of approximately 15–20 kcal/mol is an inherent and well-studied property of planar amides.^{1–4} Geometrical distortions of the amide bond lead to disruption of the $n_N \rightarrow \pi^*_{C=O}$ delocalization, which results in lower barriers to cis–trans isomerization of amides.^{13d–j} This effect can have profound implications for the reactivity of amide bonds.¹⁰ Despite the importance of resonance energies, few studies probing the effect of resonance on the physicochemical properties of nonplanar amides have been reported.²⁴ The lack of theoretical studies hampers the understanding of the chemical consequences of amide bond distortion and inhibits the rational design of new analogues.

Several methods for the calculation of resonance energies of amide bonds have been described in the literature.^{3h,24b} In the present study, isodesmic equations utilizing the carbonyl substitution nitrogen atom replacement (COSNAR) method have been used to calculate resonance energies (REs) of one-carbon-bridged lactams (eq 1).^{24a,b} There are several advantages of the COSNAR approach. First, this method has been shown to be the most accurate in predicting resonance energies of strained amide bonds.^{24b} Furthermore, this method provides calculated structures and energies of the corresponding amines, ketones, and hydrocarbons, which are available for detailed examination of the structural changes that occur during the amide bond rotation in comparison with standard amide bond analogues.

$$-RE = E_{T(\text{amide})} - [E_{T(\text{amine})} + E_{T(\text{ketone})} - E_{T(\text{hydrocarbon})}] \quad (1)$$

Resonance in One-Carbon-Bridged Lactams. Table 3 lists the resonance energies together with values including zero-point energy and thermal corrections for one-carbon-bridged lactams calculated in the current study. Total energies for all of the compounds calculated in the present study with zero-point energy and thermal corrections are listed in the SI. The data in Table 3 show that the parent one-carbon-bridged lactams (Figure 3A) can be comfortably classified into three groups: (i) lactams in which the resonance virtually disappears or is very low (the [2.2.1] (2.7 kcal/mol), [3.2.1] (4.2 kcal/mol), [3.3.1] (1.4 kcal/mol), and [4.4.1] (5.1 kcal/mol) ring systems); (ii) lactams in which the resonance is calculated to be moderate, with values around 10 kcal/mol (the [4.2.1] (10.7 kcal/mol), [4.3.1] (9.6 kcal/mol), [5.4.1] (9.7 kcal/mol), and [6.3.1] (9.4 kcal/mol) ring systems); and (iii) lactams in which the resonance is calculated to be around 16–18 kcal/mol, which corresponds to a typical amide bond (the [5.2.1] (18.0 kcal/mol), [5.3.1] (16.0 kcal/mol), and [6.2.1] (16.9 kcal/mol) ring systems). In addition, the resonance energy of the azetidine-

Table 3. Resonance Energies (RE) Calculated using Carbonyl Substitution Nitrogen Atom Replacement Method (COSNAR) (MP2/6-311++G(d,p))^a

entry	amide	ring system	-RE [kcal/mol]	-RE (corr) [kcal/mol]
1	A	[2.2.1]	-2.46	-2.70
2	B	[3.2.1]	-4.14	-4.23
3	C	[3.3.1]	-1.16	-1.35
4	D	[4.1.1]	-13.87	-13.51
5	E	[4.2.1]	-10.97	-10.65
6	F	[4.3.1]	-9.81	-9.60
7	G	[4.4.1]	-5.25	-5.14
8	H	[5.2.1]	-18.65	-18.00
9	I	[5.3.1]	-16.36	-15.96
10	J	[6.2.1]	-18.10	-16.91
11	K	[5.4.1]	-10.11	-9.67
12	L	[6.3.1]	-10.23	-9.38
13	M	[4.2.1]	-10.96	-10.74
14	N	[4.3.1]	-7.31	-7.15
15	O	[4.4.1]	-5.55	-5.43
16	P	[5.2.1]	-19.55	-18.94
17	Q	[5.3.1]	-12.31	-12.02
18	R	[6.2.1]	-19.06	-18.37
19	S	[5.3.1]	-5.97	-6.21
20	T	[5.3.1]	-15.02	-14.53
21	U	[5.3.1]	-16.14	-15.64
22	V	[4.3.1]	-3.67	-3.76
23	W	[4.3.1]	-4.02	-4.07
24	X	[4.3.1]	-4.55	-4.64
25	Y	[4.3.1]	-10.20	-9.97
26	Z	[4.3.1]	-10.97	-10.75
27	AA	[4.3.1]	-11.53	-11.33
28	AB	[4.3.1]	-10.28	-10.05

^aUncorrected values and values with zero-point energy and thermal corrections are presented. Total energies of optimized structures calculated in the current study including zero-point energy and thermal corrections (MP2/6-311++G(d,p)) are listed in the SI (Table SI-1). See Figure 3 for structures A–AB.

containing bridged scaffold [4.1.1] was calculated to be 13.5 kcal/mol, which is in agreement with the resonance energies of other nonbridged β -lactams and penicillins.^{3h}

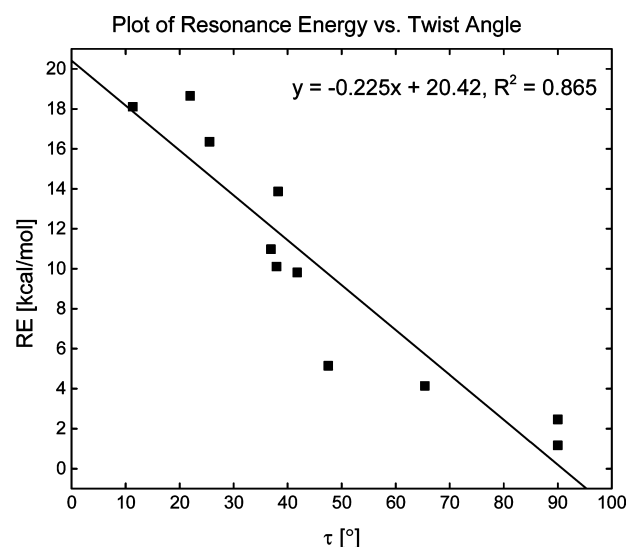
The calculated resonance energies for the advanced ring systems containing endocyclic olefins and the substituted [4.3.1] scaffolds (Figure 3B,C) follow the trend expected from their geometric properties (vide supra, Table 2). There are two interesting points that deserve a comment: (i) almost a complete disappearance of resonance energy in the tricyclic [4.3.1] bridged systems (3.8–4.6 kcal/mol) (cf. bicyclic [4.3.1] bridged systems, with resonance energies of approximately 10 kcal/mol) and (ii) minimal influence of the substituents at the α -position on the resonance energy (9.6–11.3 kcal/mol). More importantly, the calculated resonance energies of the tricyclic amides provide an explanation for the reactivity differences observed experimentally.^{33–35}

Relationship between Resonance and Amide Bond Geometry. The present study verifies the effect of amide bond geometry on the resonance energies as a function of N–C(O) rotation. The following points are noteworthy:

(1) There appears to be a negative linear relationship between the resonance energy and the N–C(O) bond twist angle (12 parent lactams, $Y = -0.204X + 19.04$, $R^2 = 0.79$; outlier analysis, [6.3.1] scaffold, $Y = -0.224X + 20.42$, $R^2 =$

0.87; Chart 3). Interestingly, a more accurate negative linear relationship is found between the resonance energy and the

Chart 3. Correlation of Resonance Energy (RE) with Twist Angle (τ) for Amides A–L^a



^aLeave-one-out analysis: the outlier, with RE = 10.2 kcal/mol and $\tau = 18.84^\circ$, represents compound L, [6.3.1]. It should be noted that leave-two-out analysis (compound G, [4.4.1]) gives $R^2 = 0.92$. For an extended plot of resonance energy versus τ , see the SI.

sum of the twist angle and pyramidalization at carbon, $\Sigma_{(\tau+\chi_c)}$, in the series (12 parent lactams, $Y = -0.228X + 21.93$, $R^2 = 0.82$; outlier analysis, [6.3.1] scaffold, $Y = -0.256X + 23.96$, $R^2 = 0.92$; not shown, see the SI)

(2) There appears to be a negative linear relationship between the resonance energy and the sum of the N–C(O) and C=O bond lengths (12 parent lactams, $Y = -0.003X + 2.66$, $R^2 = 0.73$; outlier analysis, [6.3.1] scaffold, $Y = -0.003X + 2.66$, $R^2 = 0.79$). However, plots of resonance energy versus the N–C(O) and C=O bond lengths reveal scattered correlations (not shown). In addition, the resonance energy gives poor correlations with the pyramidalization at nitrogen and the pyramidalization at carbon.

Overall, these findings suggest that in the studied family of lactams the loss of resonance energy is predominantly determined by the twist of the N–C(O) bond rather than by variations in the pyramidalization at nitrogen toward sp^3 hybridization. Interestingly, in the series of 2-quinclidones with extended ring systems previously reported by Greenberg^{24b} there appears to be a good correlation between the loss of resonance energy and the pyramidalization at nitrogen (nine lactams, $Y = 0.383X - 1.53$, $R^2 = 0.86$; not shown) but not between the loss of resonance energy and the twist angle. The fact that two different structural parameters can be correlated with the resonance energy in these systems suggests that the twist angle and the pyramidalization at nitrogen are the respective major contributors to the factors governing the amide bond distortion in these amides. Further studies will focus on elucidating the origin of structural differences in nonplanar lactams.

Protonation Sites and Proton Affinities. As predicted by the resonance theory, planar amides undergo protonation at oxygen (e.g., formamide: O-protonation is favored over N-

Table 4. Total Energies and Selected Geometric Parameters for Optimized Structures of N- and O-Protonated Bridged Amides Calculated at the MP2/6-311++G(d,p) Level^a

entry	amide	$-E_T$ [au]	$-E_T$ (corr) [au]	N–C(O) [Å]	C=O [Å]	τ [deg]	χ_N [deg]	χ_C [deg]
1	A-NH ⁺	363.43156	363.26356	1.605	1.178	90.00	66.46	0.00
	A-OH ⁺	363.37084	363.20378	1.388	1.266	90.00	72.05	0.01
2	B-NH ⁺	402.64500	402.44620	1.569	1.185	73.13	59.56	1.52
	B-OH ⁺	402.60627	402.40841	1.336	1.299	51.13	57.78	18.94
3	C-NH ⁺	441.84667	441.61699	1.545	1.193	90.00	50.02	0.00
	C-OH ⁺	441.80491	441.57657	1.332	1.308	54.89	48.50	22.80
4	D-NH ⁺	402.61759	402.42005	1.624	1.173	48.46	61.79	0.72
	D-OH ⁺	402.59522	402.39749	1.319	1.299	32.41	46.64	12.33
5	E-NH ⁺	441.84203	441.61286	1.577	1.186	50.27	54.68	0.37
	E-OH ⁺	441.82949	441.60064	1.308	1.309	31.69	37.31	17.74
6	F-NH ⁺	481.03828	480.77865	1.558	1.194	58.70	49.37	1.42
	F-OH ⁺	481.03090	480.77188	1.306	1.319	37.15	25.34	21.34
7	G-NH ⁺	520.24115	519.95125	1.551	1.197	67.87	46.14	1.04
	G-OH ⁺	520.22374	519.93443	1.310	1.322	38.53	29.91	20.99
8	H-NH ⁺	481.03737	480.77806	1.585	1.186	29.47	50.50	0.07
	H-OH ⁺	481.04575	480.78644	1.303	1.314	20.90	22.42	10.73
9	I-NH ⁺	520.23223	519.94247	1.557	1.195	64.53	48.29	1.50
	I-OH ⁺	520.23919	519.94961	1.302	1.319	22.69	13.42	12.44
10	J-NH ⁺	520.22450	519.93517	1.579	1.187	14.97	49.82	2.08
	J-OH ⁺	520.24525	519.95557	1.299	1.315	10.92	6.32	5.02
11	K-NH ⁺	559.42582	559.10551	1.547	1.199	82.69	44.59	3.21
	K-OH ⁺	559.42406	559.10411	1.305	1.323	28.36	3.45	12.98
12	L-NH ⁺	559.42364	559.10367	1.578	1.193	24.19	47.27	5.57
	L-OH ⁺	559.44407	559.12408	1.301	1.324	15.09	1.39	5.98
13	M-NH ⁺	440.62131	440.41706	1.575	1.186	48.06	55.89	1.84
	M-OH ⁺	440.61051	440.40658	1.310	1.306	28.44	42.40	15.65
14	N-NH ⁺	479.82019	479.58548	1.545	1.195	68.23	50.35	3.00
	N-OH ⁺	479.80774	479.57345	1.306	1.319	35.84	33.18	19.61
15	O-NH ⁺	519.01747	518.75232	1.548	1.195	64.69	48.49	0.48
	O-OH ⁺	518.99831	518.73380	1.309	1.320	37.56	32.33	20.99
16	P-NH ⁺	479.80429	479.56968	1.590	1.184	26.87	50.94	1.47
	P-OH ⁺	479.81256	479.57778	1.303	1.311	17.00	27.05	10.78
17	Q-NH ⁺	519.02103	518.75617	1.575	1.191	47.34	45.00	2.16
	Q-OH ⁺	519.02379	518.75900	1.307	1.315	30.69	20.50	10.96
18	R-NH ⁺	519.00978	518.74513	1.573	1.188	33.60	50.55	0.07
	R-OH ⁺	519.01927	518.75443	1.301	1.316	20.20	12.63	11.16
19	S-NH ⁺	519.00486	518.74024	1.574	1.191	51.78	45.85	0.41
	S-OH ⁺	519.01272	518.74859	1.306	1.315	25.34	17.27	12.34
20	T-NH ⁺	519.01199	518.74697	1.559	1.194	43.97	46.76	0.31
	T-OH ⁺	519.01626	518.75117	1.302	1.319	23.97	20.94	13.05
21	U-NH ⁺	519.01040	518.74538	1.552	1.194	41.18	49.11	4.80
	U-OH ⁺	519.02031	518.75545	1.302	1.320	29.21	14.12	13.04
22	V-NH ⁺	597.44182	597.11466	1.541	1.196	73.07	48.11	2.46
	V-OH ⁺	597.42070	597.09439	1.311	1.320	46.12	30.26	20.05
23	W-NH ⁺	596.23063	595.92835	1.550	1.195	72.41	47.83	1.72
	W-OH ⁺	596.20966	595.90816	1.311	1.319	45.87	29.57	19.54
24	X-NH ⁺	635.43324	635.10145	1.556	1.196	70.17	46.65	1.87
	X-OH ⁺	635.41439	635.08352	1.312	1.320	45.27	28.48	18.43
25	Y-NH ⁺	520.24121	519.95240	1.562	1.195	57.93	48.50	1.54
	Y-OH ⁺	520.23477	519.94666	1.307	1.319	37.42	24.42	20.96
26	Z-NH ⁺	633.31598	633.01643	1.556	1.197	55.12	49.60	3.19
	Z-OH ⁺	633.32471	633.02569	1.314	1.298	37.76	24.76	20.09
27	AA-NH ⁺	595.29074	594.99640	1.565	1.192	61.91	47.94	0.91
	AA-OH ⁺	595.28062	594.98700	1.307	1.320	38.26	21.88	23.64
28	AB-NH ⁺	917.89975	917.60847	1.570	1.193	58.03	48.18	2.71
	AB-OH ⁺	917.90101	917.61009	1.307	1.311	37.36	24.17	20.76

^aIn all of the O-protonated structures, the proton is attached trans to nitrogen (see Figure 6). For X-ray data on N-protonated derivatives of E, see ref 34a. For computational data on protonated 2-quinclidone derivatives, see ref 24a,b. For X-ray data on O-protonated dimethylacetamide hydrochloride, see ref 46f. See Figure 3 for structures A–AB.

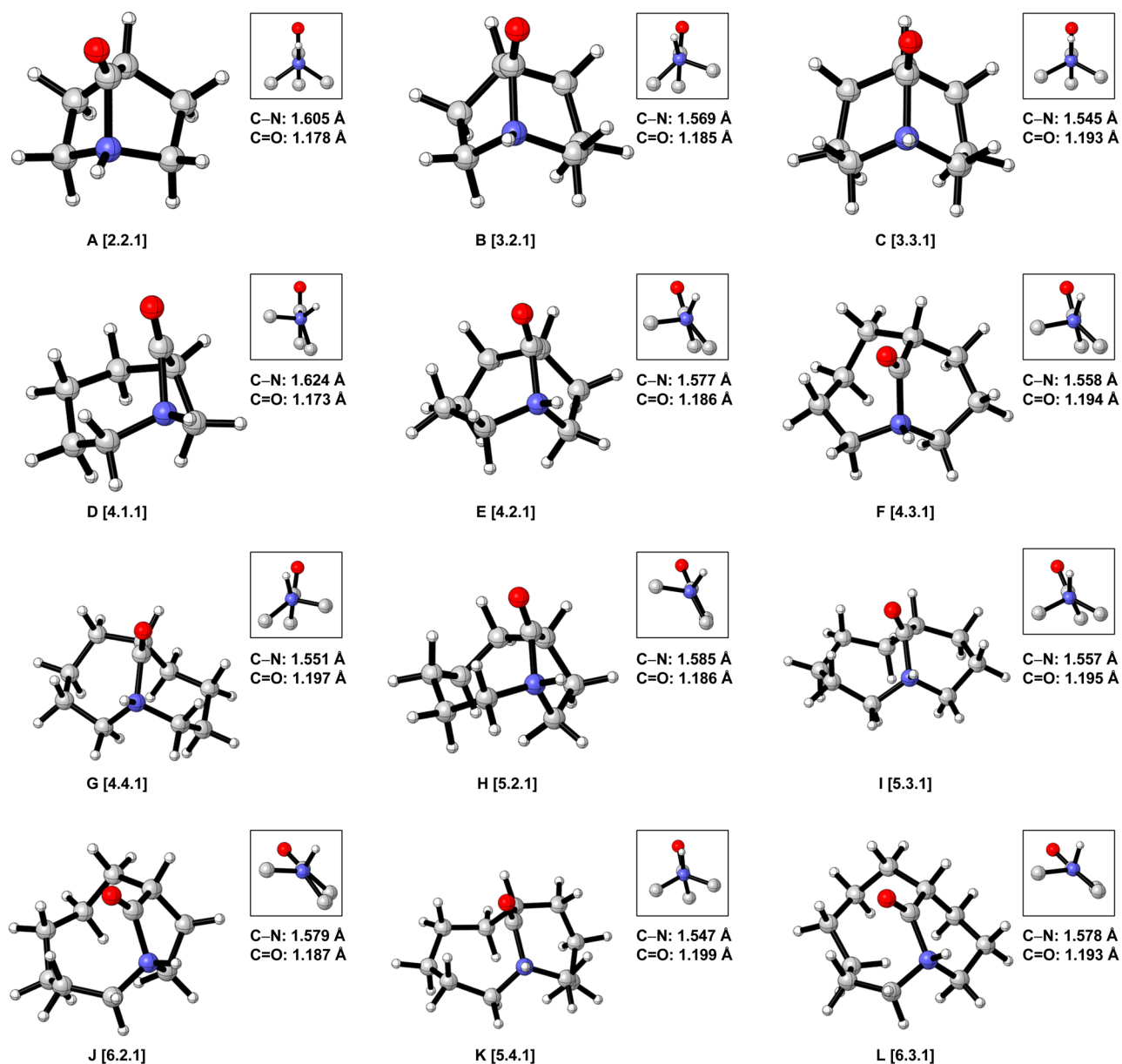


Figure 5. Optimized geometries of N-protonated bridged lactams A–L (MP2/6-311++G(d,p)). The insets show Newman projections along the N–C(O) axis. For clarity, the Newman projections are presented in the same orientation as the lactam geometries. Bond lengths are given in Å. For optimized geometries (Cartesian coordinates) of N-protonated lactams M–AB (MP2/6-311++G(d,p)) see the SI. See Figure 3 for structures A–L.

protonation by ca. 11.5 kcal/mol).^{1–4} O-protonation of planar amides shortens the N–C(O) bond and significantly reinforces the double-bond character of amides (the RE of O-protonated amides is ca. 40 kcal/mol).⁴⁶ The design and isolation of N-protonated amides has been considered a major challenge in organic synthesis.³⁴ N-protonation of amides is critical in numerous biological processes, including amide bond proteolysis^{13a–c} and protein folding,^{13d–f} as well as in organic synthesis as a method to activate amide bonds toward novel reactivity.^{33,34} N-Protonation of amides has been shown to result in disruption of the amide bond resonance,⁴⁷ which can be used to catalyze the isomerization of amide bonds and to promote reactions of C–N bonds adjacent to the carbonyl group in amides. Previous studies demonstrated that nonplanar amides characterized by the approximate distortion parameters $\tau = 20^\circ$, $\chi_N = 50^\circ$ (for a 1-azabicyclo[3.3.1]nonan-2-one derivative)^{34b} and $\tau = 50^\circ$, $\chi_N = 30^\circ$ (for derivatives of a [4.3.1]

ring system)^{34a} are predominantly protonated at nitrogen. At present, the structural factors that govern the N- versus O-protonation aptitude in amides are poorly understood.

Total energies of N- and O-protonated one-carbon-bridged twisted lactams together with values including zero-point energy and thermal corrections as well as selected structural parameters are listed in Table 4. The optimized geometries of the N- and O-protonated parent lactam ring systems (Figure 3A) as well as Newman projections along the N–C(O) axis illustrating changes that occur during protonation of the amide bonds are presented in Figure 5 (N-protonation) and Figure 6 (O-protonation). Cartesian coordinates for all of the computed N- and O-protonated structures (Figure 3B,C) are presented in the SI. For all of the O-protonated lactams, the proton was attached trans to nitrogen following the published X-ray data for O-protonated dimethylacetamide (DMA)^{46f} and previous studies.^{24a,b}

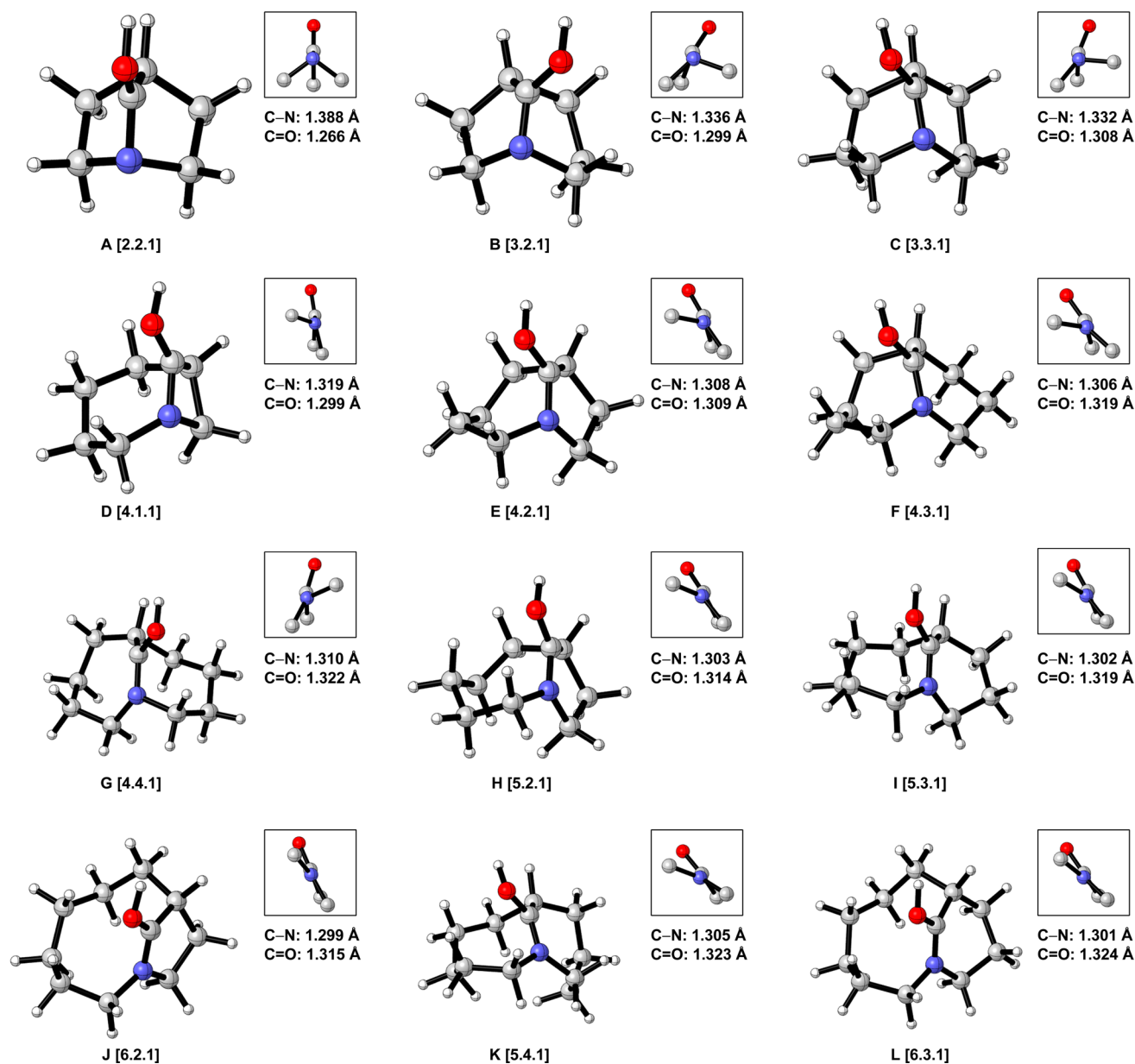


Figure 6. Optimized geometries of O-protonated bridged lactams A–L (MP2/6-311++G(d,p)). The insets show Newman projections along the N–C(O) axis. For clarity, the Newman projections are presented in the same orientation as the lactam geometries. Bond lengths are given in Å. For optimized geometries (Cartesian coordinates) of O-protonated lactams M–AB (MP2/6-311++G(d,p)), see the SI. See Figure 3 for structures A–L.

N- and *O*-Protonated One-Carbon Bridged Lactams. Examination of the data in Table 4 leads to several important observations. Notably, *N*-protonation results in a significant lengthening of the N–C(O) bond (12 parent lactams, $\Delta = 0.099$ – 0.214 Å, average lengthening of 0.169 Å), while the C=O bond undergoes moderate shortening (12 parent lactams, $\Delta = 0.019$ – 0.041 Å, average shortening of 0.031 Å). The increase in the N–C(O) bond length is due to several effects: (i) the large covalent radius of quaternized nitrogen (the adjacent C–N bonds undergo substantial lengthening by averages of 0.042 and 0.049 Å, respectively);⁴⁸ (ii) a substantial increase in the pyramidal character of the nitrogen atom (all amides in the series contain essentially pyramidalized nitrogen atoms: $\chi_N = 44.6$ – 66.5° ; average increase of 14.7°).²⁴ The most pronounced effect is observed in amides that are less distorted in the ground state (e.g., J, [6.2.1] experiences an impressive increase in the χ_N value from 6.0° to 49.8° , $\Delta = 43.8^\circ$), as

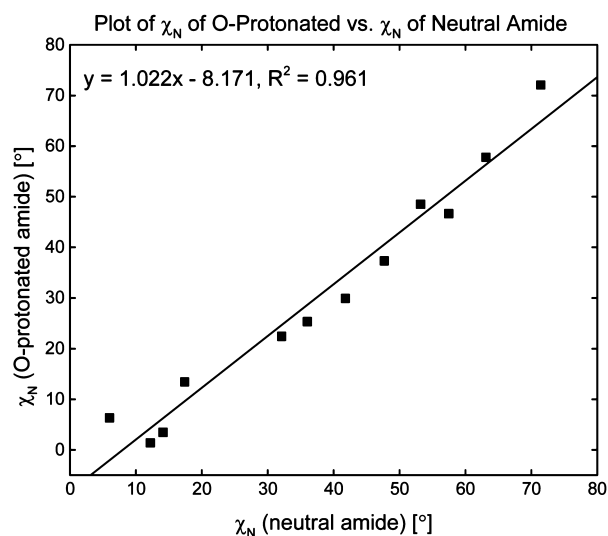
expected. Changes in the pyramidalization at nitrogen are followed by rotation around the N–C(O) axis (an average increase in the twist angle of 14.1° , with the [5.3.1] and [5.4.1] ring systems experiencing the most dramatic increases in distortion: $\Delta\tau = 39.0^\circ$ and $\Delta\tau = 44.8^\circ$, respectively). Taken together, these effects result in a net increase in the distortion of *N*-protonated amide bonds.

Moreover, significant changes are observed with regard to the amide bond geometry. Most importantly, the C–C–O angle dramatically opens ($\Delta = 6.6$ – 9.9° , average of 8.2°), while the N–C–O angle significantly closes ($\Delta = 3.9$ – 8.4° , average of 6.0°).⁴⁹ These effects are consistent with the beginning of collapse of the N–C(O) bond upon *N*-protonation. A comprehensive list of N–C–O and C–C–O angles as well as other geometric parameters for all of the studied *N*- and *O*-protonated lactams is presented in the SI (Tables SI-3A and SI-3B).

Table 4 reveals that O-protonation of the studied amides results in a considerable lengthening of the C=O bond (12 parent lactams, $\Delta = 0.065\text{--}0.099$ Å, average lengthening of 0.090 Å), while the N–C(O) bond shortens to a similar extent ($\Delta = 0.066\text{--}0.114$ Å, average shortening of 0.087 Å). In eight of the O-protonated lactams, the C=O bond is longer than the N–C(O) bond, which provides compelling support for the amide bond resonance theory (Table 4, entries 5–12).^{1–4} A moderate decrease in the pyramidalization at nitrogen (average loss of 7.3°) and the twist angle (average loss of 7.6°) was calculated for O-protonated amides in comparison with neutral amides (a dramatic difference in the pyramidalization at nitrogen and the twist angle between N- and O-protonated lactams can be seen in Table 4). This effect is consistent with a net decrease in the amide bond distortion to enhance the $n_{\text{N}} \rightarrow \pi^*_{\text{C=O}}$ conjugation during O-protonation,⁴⁶ and with previous studies.²⁴ O-Protonated amides are more stable than neutral amides (RE of 35–45 kcal/mol vs RE of 15–20 kcal/mol).^{24,46} Additionally, significant geometric effects are observed upon O-protonation. In the O-protonated structures, the N–C–O angle is closed dramatically ($\Delta = 4.8\text{--}6.6^\circ$, average of 5.7° vs neutral amides) while the C–C–O angle remains practically unchanged ($\Delta = -1.3$ to 3.1°, average of 0.7°), consistent with the enhanced $n_{\text{N}} \rightarrow \pi^*_{\text{C=O}}$ resonance stabilization in O-protonated amides in the series.⁴⁹

Interestingly, a plot of the pyramidalization at nitrogen in the O-protonated amides versus the pyramidalization at nitrogen in the neutral amides gives a linear correlation (12 parent lactams, $Y = 1.022X - 8.17$, $R^2 = 0.96$; Chart 4). Similarly, there appears

Chart 4. Correlation of the Pyramidalization at Nitrogen in the O-Protonated Amides ($\chi_{\text{N,OH}^+}$) with the Pyramidalization at Nitrogen in the Neutral Amides (χ_{N}) for amides A–L (For an Extended Plot of $\chi_{\text{N,OH}^+}$ versus χ_{N} , See the SI)



to be a good correlation between the twist angles in the O-protonated and neutral amides (12 parent lactams, $Y = 0.775X + 2.18$, $R^2 = 0.87$; not shown, see the SI). The analogous correlations employing N-protonated amides give scattered results ($R^2 = 0.64$ and 0.71, respectively; not shown). In addition, a plot of the difference in the pyramidalizations at nitrogen in the N- and O-protonated amides, $\Delta(\chi_{\text{N,NH}^+} - \chi_{\text{N,OH}^+})$ versus the pyramidalization at nitrogen in the neutral amides (χ_{N}) gives an accurate linear correlation for this series of amides

(12 parent lactams, $Y = -0.772X + 51.1$, $R^2 = 0.94$; not shown, see the SI). The latter effect is indicative of the more pronounced changes in the geometry upon N-protonation in amides that are less distorted in the ground state.

In summary, these results provide insight into the changes that occur upon N- vs O-protonation of amide bonds. N-Activation severely disrupts the amide resonance, while O-protonation enhances the planarity of amide bonds in the series of one-carbon-bridged lactams. These findings validate previous experimental observations on the role of N-protonation,^{10a} including activation of moderately distorted amides,^{33,34a,31a} and provide another argument to verify the classical amide bond resonance theory.^{3a,24a,b}

Proton Affinities. Table 5 lists proton affinity (PA) values and differences between the N- and O PAs (ΔPA) for the series

Table 5. Proton Affinities (PA) and Differences in Proton Affinities (ΔPA) [in kcal/mol] Calculated for One-Carbon-Bridged Lactams at the MP2/6-311++G(d,p) Level^a

entry	amide	uncorrected			corrected		
		PA _N	PA _O	ΔPA	PA _N	PA _O	ΔPA
1	A	232.9	194.8	38.1	223.9	186.4	37.5
2	B	233.6	209.3	24.3	224.6	200.9	23.7
3	C	237.3	211.1	26.2	227.9	202.6	25.4
4	D	227.3	213.2	14.0	218.7	204.6	14.2
5	E	227.9	220.0	7.9	219.1	211.5	7.7
6	F	229.7	225.0	4.6	220.7	216.4	4.3
7	G	234.6	223.7	10.9	225.5	215.0	10.6
8	H	220.3	225.6	-5.3	211.8	217.0	-5.3
9	I	224.0	228.4	-4.4	215.2	219.7	-4.5
10	J	214.4	227.4	-13.0	206.0	218.8	-12.8
11	K	229.8	228.7	1.1	220.7	219.8	0.9
12	L	217.9	230.7	-12.8	209.27	222.0	-12.8

^aFor an extended table, see the SI. Uncorrected values and values with zero-point energy and thermal corrections are presented. For calculated proton affinities of 2-quinolidone derivatives, see ref 24a,b. For experimental studies on N-protonation of nonplanar amides, see ref 34a. For experimental studies on N-methylation of nonplanar amide bonds, see refs 17b, 18, 34a, and 44. See Figure 3 for structures A–L.

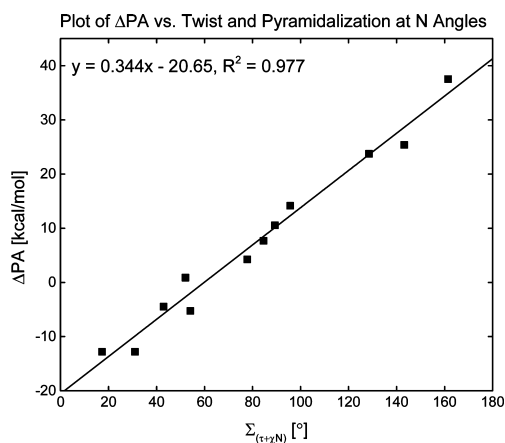
of studied lactams together with values including zero-point energy and thermal corrections.^{24,46} The absolute N and O PA values differ by approximately 8.7 kcal/mol after zero-point energy and thermal corrections, but the proton affinity differences (ΔPA) are similar (average difference of 0.25 kcal/mol) for the corrected and uncorrected values, in accord with previous studies.^{24b} In the series of parent lactam scaffolds, the highest proton affinity was calculated for N-protonation of the [3.3.1] ring system, consistent with the nitrogen atom in this scaffold being the most basic and its reactive properties as an amino-ketone equivalent.^{31e} The lowest proton affinity was found for O-protonation of the [2.2.1] ring system, which is in agreement with the highly strained amide bond in this lactam.^{31g}

A detailed analysis of the results in Table 5 reveals that the studied lactams can be divided into two groups: (i) amides that favor protonation at nitrogen ($\Delta\text{PA} = 4.3\text{--}37.5$ kcal/mol: scaffolds A–G, [2.2.1], [3.2.1], [3.3.1], [4.1.1], [4.2.1], [4.3.1]), and (ii) amides that favor O-protonation ($\Delta\text{PA} = -4.5$ to -12.8 kcal/mol: scaffolds H–J and L, [5.2.1], [5.3.1], [6.2.1], [6.3.1]). An exception is the [5.4.1] ring system (scaffold K),

which is calculated to favor N-protonation by only 0.9 kcal/mol. This ring system is predicted to undergo both O- and N-protonation close to equilibrium.^{24a} The first three amides in the series (the [2.2.1], [3.2.1], and [3.3.1] ring systems) favor N-protonation over O-protonation by 24–38 kcal/mol, which compares favorably with the Δ PA value of 22.8 kcal/mol determined earlier for the perpendicular 2-quinuclidone^{19,24a} as well as with the Δ PA value of 26.3 kcal/mol calculated for 2-quinuclidone at the MP2/6-311++G(d,p) level. Four other ring systems calculated in the current study (the [4.1.1], [4.2.1], [4.3.1], and [4.4.1] ring systems) favor N-protonation over O-protonation by 4.3–14.1 kcal/mol, which compares favorably with Δ PA value of 1.4 kcal/mol determined earlier for 1-azabicyclo[3.3.1]nonan-2-one.^{24a,34b}

The crossover point from N- to O-protonation in the studied series of lactams is located around the geometry region defined by the [5.4.1] ring system. *There is an excellent linear correlation between Δ PA and the sum of the twist angle and the pyramidalization at nitrogen* (12 parent lactams, $Y = 0.34X - 20.65$, $R^2 = 0.98$, Chart 5; all lactams, $Y = 0.35X - 22.32$, $R^2 =$

Chart 5. Correlation of Δ PA with the Sum of the Twist Angle and Pyramidalization at Nitrogen, $\Sigma_{(\tau+\chi_N)}$ for amides A–L (For an Extended Plot of Δ PA versus $\Sigma_{(\tau+\chi_N)}$, See the SI)



0.97, see the SI), which can be compared with the correlation between Δ PA and the twist angle (12 parent lactams, $Y = 0.577X - 17.88$, $R^2 = 0.90$; not shown, see the SI) and the correlation between Δ PA and the pyramidalization at nitrogen (12 parent lactams, $Y = 0.67X + 17.93$, $R^2 = 0.86$; not shown, see the SI). This finding validates the use of additive descriptors of the geometric transformations of amide bonds to predict reactive properties of nonplanar amides (vide supra). Importantly, this equation provides a very useful tool to predict N- versus O-protonation sites of twisted amides, as only a single determination of the amide bond geometry from X-ray crystallography or calculations is needed to provide a reliable prediction of Δ PA.^{3,4} Since our calculations have already shown that $\Sigma_{(\tau+\chi_N)}$ can be correlated with the N–C(O) bond length (vide supra), this can be used in conjunction with amide bond distortion parameters to accurately predict Δ PA in one-carbon-bridged amides. Overall, this finding provides a compelling answer to the long-standing question of structural factors governing the N- versus O-protonation switch in nonplanar lactams and determines

that a $\Sigma_{(\tau+\chi_N)}$ value of ca. 50–60° should be sufficient to promote N-protonation of amides.^{1–4,10–12,24,33–35}

Interestingly, there appears to be a more accurate correlation between the proton affinity at oxygen and the pyramidalization at nitrogen ($Y = -0.44X + 228$, $R^2 = 0.81$; not shown) or the twist angle ($Y = -0.35X + 227$, $R^2 = 0.73$; not shown) in neutral amides than between the proton affinity at nitrogen and the pyramidalization at nitrogen ($Y = 0.23X + 210$, $R^2 = 0.55$; not shown) or the twist angle ($Y = 0.23X + 209$, $R^2 = 0.73$, not shown) in neutral amides, including additive parameters ($R^2 = 0.85$ vs $R^2 = 0.71$; not shown), which could indicate that the loss of oxygen basicity is the major factor contributing to the reactivity of these amides. It should be noted that strain in smaller bridgehead bicyclic ring systems, charge dispersion, and solvent effects may also contribute to the relative proton affinities in synthetic studies^{24,25}. Solvent effects have been shown to enhance the ability of oxygen to undergo protonation as a result of steric effects.^{3,24,25}

Analysis of the proton affinities of the advanced ring systems of bridged lactams containing endocyclic olefins^{31a} and substituted [4.3.1] ring systems^{28,31b,c,33–35} (Figure 3B,C) leads to several important observations. First, a significant increase in favor of N- versus O-protonation was calculated for olefin-containing bridged lactams in comparison with their saturated analogues (cf. the [4.3.1] and, in particular, [6.2.1] ring systems). Second, a dramatic increase in favor of N-protonation was calculated for amide bonds embedded in tricyclic [4.3.1] ring systems in comparison with simple bicyclic [4.3.1] ring system analogues (tricyclic amides favor N-protonation over O-protonation by ca. 13–14 kcal/mol vs 4–5 kcal/mol for bicyclic amides). Third, polar substituents (R) placed at the α -position in the [4.3.1] ring system show a strong activating effect (R = OMe, 6.4 kcal/mol) or a very strong deactivating effect (R = C(O)Me, –5.5 kcal/mol; R = SMe, –0.8 kcal/mol) on the adjacent nonplanar amide bonds toward N- versus O-protonation. These effects result from the following geometric features:

- The higher affinity for N-protonation in the olefin-containing and tricyclic systems is consistent with the increased rigidity of these rings, which results in enhanced distortion of the amide linkage.^{34a} The high proton affinities at nitrogen are likely to contribute to the enhanced reactivity of these amides observed experimentally;²⁸ however, an explanation for this effect has remained elusive to date.
- The effect of polar substituents at the α -position results from inductive effects and the presence of an internal hydrogen bond and is consistent with the reactivity of these amides observed experimentally. For example, degradation of α -OMe-containing twisted amides has been noted during their synthesis,^{31b} while the structurally homologous α -SMe-substituted lactams have been found to be robust toward storage and isolation conditions.^{31b} Differences in the stability of α -carbonyl-containing bridged lactams have also been noted.^{31a,c,35}

Overall, these findings demonstrate that modification of the relative proton affinity values by substituents placed in close proximity to the amide bond should be considered when designing new analogues of nonplanar amides.

In summary, the analysis of proton affinities indicates that one-carbon-bridged lactams are well-suited for elucidation of

the structural requirements for the O- versus N-protonation switch because the crossover point is clearly defined in this series. Notably, a plot of ΔPA versus the sum of the twist angle and pyramidalization at nitrogen reveals an excellent linear correlation, which determines that distortion of an amide linkage by about 30–40% from the maximum value (ca. 50–60° out of 150°) should be sufficient to promote N-protonation reactions in this series. The calculated ΔPA values in the series indicate that new ring systems of one-carbon-bridged lactams may participate in the intriguing N-protonation (N-activation) reactions.⁵⁰ These findings should facilitate further synthetic applications of nonplanar amides.

Core Ionization Energies and Atomic Charges. As predicted by the resonance theory, distortion of amides should decrease the contribution of the polar resonance form, leading to more negative nitrogen, more positive oxygen, and more positive carbon atoms in nonplanar amides compared with planar amides.^{2–4} Determination of the charges at N, O, and C in nonplanar amides is expected to facilitate prediction of the reactive properties of twisted amides.^{3,24}

Calculated core ionization energies⁵¹ and atomic charges⁵² of the studied one-carbon-bridged lactams are listed in Tables 6 and 7, respectively. Experimental studies to determine the core ionization energies of one-carbon-bridged twisted lactams have not been reported to date.^{51a} The aims of determining charges in the current study were as follows: (i) to compare the core ionization energies of one-carbon-bridged lactams with the previously reported values for 2-quinuclidone derivatives;^{24a,b} (ii) to elucidate a correlation with the geometric parameters of nonplanar lactams to test the validity of the classical resonance model;^{1–4} and (iii) to determine whether atomic charges could serve as a useful tool in predicting the reactive properties of one-carbon-bridged twisted amides.^{3a}

Core Ionization Energies. Examination of the data in Table 6 reveals several points. The highest O 1s ionization energies (least negative O) were calculated for amides A–C, in which the contribution from the polar resonance form is geometrically prohibited. In agreement with the geometric argument, lactams A–C have the highest C 1s ionization energies (most positive C); however, there is no apparent correlation between the N 1s

ionization energy and the $n_{\text{N}} \rightarrow \pi^*_{\text{C=O}}$ conjugation, with the lowest N 1s (least positive N) calculated for the [4.4.1] ring system.^{24a,b}

A more detailed analysis reveals several noteworthy features: (1) A plot of the C 1s ionization energy versus the O 1s ionization energy gives a linear correlation (12 parent lactams, $Y = 0.805X + 138.5$, $R^2 = 0.88$; Chart 6A). (2) Interestingly, plots of the N 1s ionization energy versus the C 1s and O 1s ionization energies give poor correlations. (3) There appears to be an excellent linear correlation between ΔPA and the O 1s orbital energy (12 parent lactams, $Y = -0.021X - 550.7$, $R^2 = 0.97$; Chart 6B). (4) In addition, there are several good linear correlations between the amide bond geometric distortion parameters and the O 1s ionization energy, including (i) O 1s ionization energy as a function of the pyramidalization at nitrogen (12 parent lactams, $Y = -0.014X - 550.3$, $R^2 = 0.84$; not shown), (ii) O 1s ionization energy as a function of the twist angle (12 parent lactams, $Y = -0.012X - 550.3$, $R^2 = 0.87$; not shown), and (iii) O 1s ionization energy as a function of the length of the N–C(O) bond (12 parent lactams, $Y = -9.54X - 537.5$, $R^2 = 0.99$; not shown). As expected, the O 1s ionization energy can be correlated with the C=O bond length (12 parent lactams, $Y = -30.6X + 588.2$, $R^2 = 0.87$; not shown), while the C 1s ionization energy can be correlated with other geometric structural parameters (vide supra). In contrast, changes in the N 1s ionization energy appear to be independent of the amide bond geometric parameters in the studied series.^{24a,b,51a}

Charges. Table 7 provides calculated natural bond orbital (NBO) atomic charges of one-carbon-bridged lactams.⁵² The data in Table 7 reveal that charges serve as good predictors of the reactive properties of nonplanar amides. The most distorted lactams, A–C, are characterized by the highest charge densities at oxygen (least negative O) in the series. There is a noticeable tendency of the charge on nitrogen to decrease toward that of the least positive N with increasing distortion within the same ring system of one-carbon-bridged lactams (cf. [3.3.1], [4.3.1], [5.3.1] and [4.2.1], [5.2.1], [6.2.1]). Thus, the calculated atomic charges in this series of lactams are consistent with the classical amide bond resonance model.^{1–4}

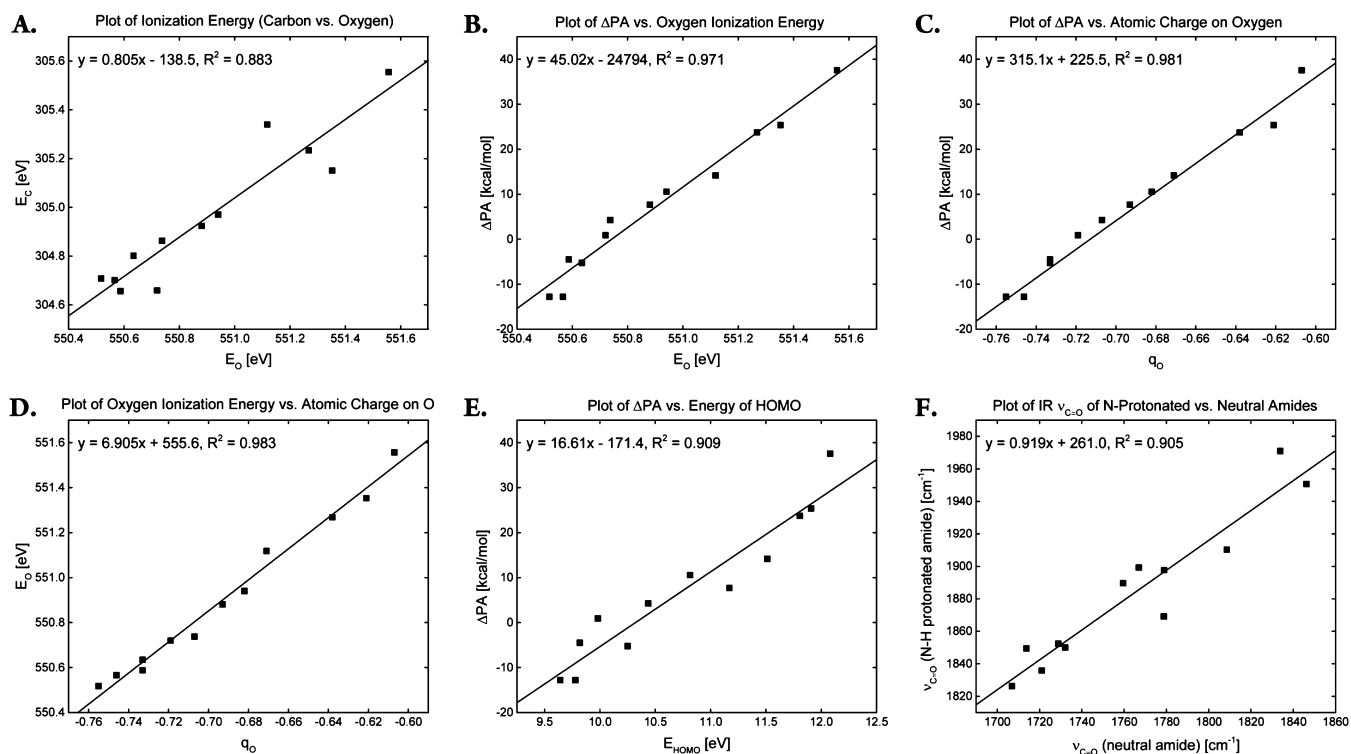
A more detailed analysis provides significant insight into the use of atomic charges for the prediction of reactive properties of nonplanar amides. Importantly, there is an excellent linear correlation between ΔPA and the charge on oxygen (q_{O}) (12 parent lactams, $Y = 0.003X - 0.715$, $R^2 = 0.98$; Chart 6C), and this simple calculation of the charge on O can be used to accurately predict protonation sites of nonplanar bridged lactams. There appear to be linear correlations between the O 1s ionization energy and q_{O} (12 parent lactams, $Y = -0.142X - 79.18$, $R^2 = 0.98$; Chart 6D) and the N 1s ionization energy and the atomic charge on nitrogen (q_{N}) (12 parent lactams, $Y = -0.083X - 35.53$, $R^2 = 0.81$; not shown, see the SI). Moreover, a plot of q_{O} versus the N–C(O) bond twist angle gives a linear correlation (12 parent lactams, $Y = 0.001X - 0.772$, $R^2 = 0.91$; not shown); however, correlations involving other geometric parameters and the charges on nitrogen and carbon appear to be scattered.

In summary, the calculated core orbital energies in the series of nonplanar one-carbon-bridged lactams are consistent with the classical resonance model, but quantification of the charges at nitrogen is more complex because of additional steric and electronic effects. Importantly, determination of the core orbital energies in the present series argues against the presence of the $\text{C}^+ - \text{O}^-$ resonance form as a significant contributor to the

Table 6. Calculated O, C, and N Core Ionization Energies for One-Carbon-Bridged Lactams at the MP2/6-311+G(d,p) Level^a

entry	amide	ionization energy [eV]		
		C 1s	O 1s	N 1s
1	A	-305.55	-551.56	-418.62
2	B	-305.23	-551.27	-418.50
3	C	-305.15	-551.35	-418.38
4	D	-305.34	-551.12	-418.77
5	E	-304.92	-550.88	-418.54
6	F	-304.86	-550.74	-418.46
7	G	-304.97	-550.94	-418.39
8	H	-304.80	-550.63	-418.71
9	I	-304.66	-550.59	-418.61
10	J	-304.70	-550.57	-418.83
11	K	-304.66	-550.72	-418.47
12	L	-304.71	-550.52	-418.80

^aFor an extended table, see the SI. For calculated core ionization energies of 2-quinuclidone derivatives, see ref 24b. For experimental studies, see ref 51a. See Figure 3 for structures A–L.

Chart 6. Energy, Proton Affinity, Charge, and IR Frequency Correlations for Amides A–L^a

^aThe following correlations are shown: (A) Correlation of carbon ionization energy (E_C) with oxygen ionization energy (E_O). Leave-two-out analysis: outliers represent compounds C, [3.3.1] and D, [4.2.1]; analysis gives $Y = 0.8354X - 155.3$, $R^2 = 0.948$. (B) Correlation of Δ PA with oxygen ionization energy (E_O). (C) Correlation of Δ PA with the atomic charge on oxygen (q_O). (D) Correlation of oxygen ionization energy (E_O) with the atomic charge on oxygen (q_O). (E) Correlation of Δ PA with the energy of the HOMO (E_{HOMO}). (F) Correlation of the carbonyl infrared frequency for neutral amides ($\nu_{C=O}$) to that for N-protonated amides ($\nu_{C=O, NH^+}$). For extended plots, see the SI.

Table 7. Calculated NBO Atomic Charges for One-Carbon-Bridged Lactams at the MP2/6-311++G(d,p) Level^a

entry	amide	q_N [e]	q_O [e]	q_C [e]
1	A	-0.640	-0.607	0.852
2	B	-0.653	-0.638	0.863
3	C	-0.668	-0.621	0.866
4	D	-0.640	-0.671	0.866
5	E	-0.653	-0.693	0.870
6	F	-0.664	-0.707	0.872
7	G	-0.667	-0.682	0.875
8	H	-0.633	-0.733	0.871
9	I	-0.648	-0.733	0.862
10	J	-0.629	-0.746	0.862
11	K	-0.673	-0.719	0.874
12	L	-0.643	-0.755	0.864

^aFor an extended table, see the SI. See Figure 3 for structures A–L.

amide bond resonance (i.e., the polarization model)¹⁴ because an excellent fit between the charge density at the oxygen atom and the N–C(O) bond twist angle has been found in the series. Finally, this study demonstrates that atomic charges may be used to accurately predict the reactive properties of nonplanar amides.

Frontier Molecular Orbitals. Table 8 lists orbital energies for the highest occupied molecular orbital (HOMO), the lowest unoccupied molecular orbital (LUMO), and the first HOMO subjacent (subj) orbital for each of the parent ring systems of one-carbon-bridged lactams addressed in the current study. Orbital energies for each of the one-carbon-bridged

Table 8. Energies of the Frontier Molecular Orbitals for One-Carbon Bridged Lactams at the MP2/6-311++G(d,p) Level^a

entry	amide	E_{HOMO} [eV]	E_{subj} [eV]	E_{LUMO} [eV]
1	A	-10.75	-11.30	0.95
2	B	-10.26	-11.31	0.94
3	C	-9.86	-11.39	0.95
4	D	-10.12	-11.35	0.93
5	E	-10.02	-11.10	0.96
6	F	-9.79	-11.07	0.97
7	G	-9.76	-11.14	0.98
8	H	-9.90	-10.99	0.98
9	I	-9.81	-10.83	0.98
10	J	-9.92	-10.90	0.98
11	K	-9.78	-10.85	1.00
12	L	-9.93	-10.88	0.97

^aFor orbital energies calculated using the natural bond orbital (NBO) method, see the SI. For graphical representations of the orbitals, see the SI. For calculated frontier molecular orbitals of 2-quinuclidone derivatives, see ref 24b. See Figure 3 for structures A–L.

lactams were also calculated using the NBO method. These energies are listed in the SI (Table SI-4). Graphical representations of the HOMOs calculated for representative lactams bearing [2.2.1], [4.3.1], and [6.3.1] scaffolds spanning the whole range of amide bond distortion are presented in Figure 7. Graphical representations of the HOMO and LUMO calculated for each of the parent ring systems of bridged lactams are presented in the SI (Figure SI-2).

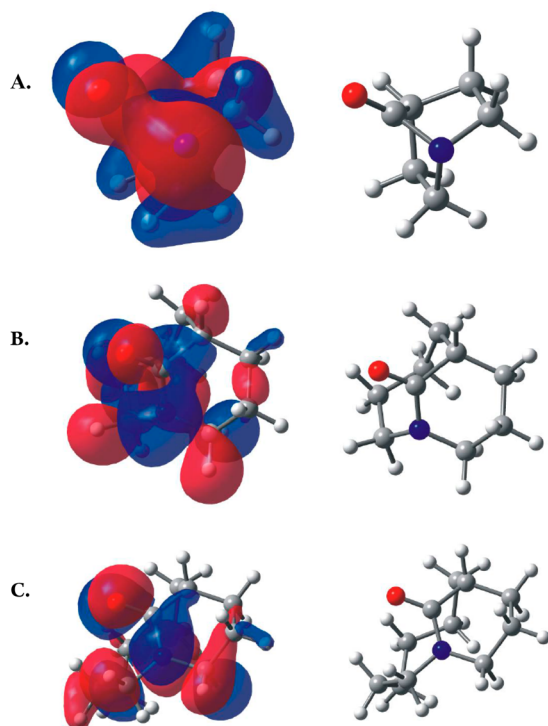


Figure 7. (left) Representations of HOMOs and (right) corresponding ball and spoke representations for representative lactams: (A) A, [2.2.1]; (B) F, [4.3.1]; (C) L, [6.3.1]. For graphical representations of the HOMOs and LUMOs of lactams A–L, see Figure SI-2.

The role of frontier molecular orbitals in the context of distortion of amide bonds has been previously investigated.^{24b,53} Rademacher determined molecular orbitals in 1-azabicyclo[3.3.1]nonan-2-one using photoelectron spectroscopy.^{53a–d} Greenberg calculated frontier molecular orbitals in unsubstituted 2-quinuclidones with extended ring systems.^{24b} Brown determined frontier molecular orbitals for benzene-fused 2-quinuclidones with gradually increasing distortion.^{53e} Brown's study suggested that distorted lactams in which the HOMO is located at an O lone pair may be protonated at oxygen, while amides in which the HOMO is located at the N lone pair may undergo protonation at nitrogen; however, this investigation was limited to four 2-quinuclidone derivatives bearing additional benzene rings, which complicated the analysis because of significant n–p mixing with aromatic rings located in close proximity to the amide bonds.

Examination of the HOMO of lactam A, [2.2.1] (Figure 7A) reveals that this orbital is dominated by n_N with a small contribution from n_O . A similar-looking HOMO was obtained for lactam F, [4.3.1] (Figure 7B) with the major contribution of electron density around the nitrogen atom; however, the contribution from n_O is significantly larger than in the fully perpendicular [2.2.1] ring system. In contrast to this, the HOMO of lactam L, [6.3.1] (Figure 7C) was calculated to be predominantly n_O in character, which is consistent with the relative distortion of the amide bond in the series. As expected, the HOMOs of other lactams in the series are positioned between the extremes defined by the [2.2.1] and [6.3.1] ring systems (Figure SI-2).

In agreement with the literature,^{24b} a closer analysis of the data in Table 8 reveals very little variation in the energies of the orbitals across the range of studied lactam geometries. For

example, the HOMO energies for the perpendicular [3.3.1] ring system, the practically planar [6.3.1] ring system, and the moderately distorted [4.3.1] scaffold were calculated to be -9.86 , -9.93 , and -9.79 eV, respectively. This flattening out effect observed in the orbital energies has been proposed to result from a significant contribution from n_N .^{24b,53,54} Interestingly, the use of NBO analysis provides a valuable quantitative description of the role of the frontier molecular orbitals on the reactivity of distorted amides across the range of nonplanar geometries in the series (see Table SI-4). Most significantly, a plot of ΔPA versus the E_{HOMO} gives a linear correlation over the range of geometries (12 parent lactams, $Y = 16.61X - 171.4$, $R^2 = 0.91$; Chart 6E). Similarly, a plot of ΔPA versus the energy difference between the HOMO and the HOMO subjacent orbitals, $\Delta(LPO-LPN)$, gives a linear correlation over the range observed (12 parent lactams, $Y = 13.40X + 12.63$, $R^2 = 0.84$; not shown, see the SI). Thus, this equation can be used to predict ΔPA if orbital energies are known from NBO calculations.

Infrared Frequencies. Table 9 lists calculated carbonyl frequencies and intensities for the one-carbon-bridged lactams

Table 9. Calculated Infrared Carbonyl Stretching Frequencies for One-Carbon-Bridged Lactams at the MP2/6-311++G(d,p) Level^a

entry	amide	$\nu_{C=O}$ (uncorr) [cm^{-1}]	$\nu_{C=O}$ (corr) [cm^{-1}]	$I_{C=O}$ [km/mol]
1	A	1846.2	1771.8	278.8
2	B	1808.6	1735.7	263.3
3	C	1778.7	1707.0	223.1
4	D	1833.8	1759.9	370.1
5	E	1778.9	1707.2	275.6
6	F	1732.1	1662.3	245.8
7	G	1721.0	1651.6	205.0
8	H	1766.9	1695.7	324.4
9	I	1728.9	1659.2	278.5
10	J	1759.5	1688.6	326.2
11	K	1706.9	1638.1	228.5
12	L	1713.8	1644.7	263.6

^aFor an extended table, see the SI. For calculated infrared carbonyl frequencies of 2-quinuclidone derivatives, see ref 24b. For experimental infrared data on nonplanar lactams, see ref 10d. For calculated infrared carbonyl frequencies of N-protonated lactams A–AB, see the SI. Correction factor = 1.042. Calculated average using literature experimental values for lactams C–J. See ref 31a. See Figure 3 for structures A–L.

examined in the current study. Historically, infrared spectroscopy has been used as one of the most valuable methods to determine the distortion of amide bonds^{17,18} because carbonyl stretching frequencies ($\nu_{C=O}$) accurately reflect changes in the local geometry of carbonyl groups and these stretches are well-isolated.⁵⁵ The frequencies of the infrared vibrations reflect the strength of the carbonyl group ($\nu_{C=O}$ increases as the C=O bond length shortens), while the intensities in the infrared spectrum are proportional to changes in the dipole moment of the carbonyl group during a vibration.⁵⁵ During amide bond rotation, the $n_N \rightarrow \pi^*_{C=O}$ overlap gradually decreases, which results in a net increase in the carbonyl stretching frequency in the infrared spectrum.^{10d} In theory, N–C(O) vibrations could also provide a valuable measurement of the changes in the amide bond resonance;^{24,55} however, these vibrations are typically mixed with other C–H and C–C vibrations, and their

analysis is not straightforward. A comprehensive study of the effect of structure and energetics on $\nu_{\text{C=O}}$ in twisted lactams has not been reported to date. For an extended discussion and additional correlations involving infrared frequencies in the studied one-carbon-bridged lactams, see the SI.

The $\nu_{\text{C=O}}$ values presented in Table 9 have been corrected using experimental data obtained for the [4.3.1] ring system of one-carbon-bridged lactams and related analogues.^{31a} A good fit between the experimental and corrected carbonyl frequencies was found for all of the studied compounds.^{24b} In the series of parent bridged lactams, with the exception of the [4.1.1] scaffold, which constitutes a special case, the highest $\nu_{\text{C=O}}$ values were calculated for the [2.2.1] and [3.2.1] rings while the lowest value was found for the [5.4.1] scaffold, which agrees well with the relative distortion parameters of the amide bonds (vide supra). Importantly, the stretching frequencies in this series cover approximately 100 cm^{-1} in the infrared spectrum (ranging from ketone-like, ca. 1800 cm^{-1} , to amide-like, ca. 1700 cm^{-1}),⁵⁵ which validates that the geometries of the studied amides span the whole range of the amide bond distortion surface.^{24b,31a} A detailed comparison of the amide bond distortion parameters with the $\nu_{\text{C=O}}$ values reveals a linear correlation between $\nu_{\text{C=O}}$ and the pyramidalization at nitrogen (12 parent lactams, $Y = 2.156X + 1677$, $R^2 = 0.80$; not shown, see the SI). Interestingly, a plot of $\nu_{\text{C=O}}$ versus the C=O bond length gives a more accurate correlation (12 parent lactams, $Y = -4155X + 6834$, $R^2 = 0.88$; not shown, see the SI).^{10d} The high carbonyl stretching frequencies observed for some of these amides verify the classic view that the attachment of N significantly changes the double bond strength in these amino-ketones (cf. the cyclobutanone $\nu_{\text{C=O}}$ stretch at ca. 1810 cm^{-1}).^{16,22c}

Infrared spectroscopy provides valuable information about geometric changes that occur upon N- and O-protonation of amides.^{34a,b} The calculated infrared frequencies of the N- and O-protonated lactams examined in the current study are presented in the SI (Table SI-5). Upon N-protonation, infrared carbonyl stretches move to higher frequencies by approximately 100 cm^{-1} (average of 119 cm^{-1}), consistent with the more ketone-like character of N-protonated amide bonds.⁴⁵ Conversely, O-protonation results in the formation of an alcohol; in these cases, a new stretching vibration appears at around 1700 cm^{-1} (average 1717 cm^{-1}) corresponding to the N=C stretch, consistent with the literature values for vibrations of imines ($\nu_{\text{C=N}}$ stretching at ca. 1640–1690 cm^{-1}).⁵⁶ A detailed analysis reveals a good correlation between the infrared carbonyl stretching frequencies of neutral and N-protonated lactams (12 parent lactams, $Y = 0.919X + 261$, $R^2 = 0.91$; Chart 6F). Moreover, plots of infrared stretching frequencies in the N-protonated amides versus geometrical parameters of the amide bond give linear correlations in the series (see the SI).

Examination of the infrared carbonyl stretching frequencies in the amide featuring an α -ketone moiety (amide Z, [4.3.1], R = C(O)Me) reveals that in the ground state the amide bond ($\nu_{\text{C=O}} = 1715 \text{ cm}^{-1}$) vibrates at an approximately 40 cm^{-1} lower frequency than the ketone moiety ($\nu_{\text{C=O}} = 1754 \text{ cm}^{-1}$), consistent with the higher electrophilicity of the carbonyl group. Upon N-protonation, the amide bond ($\nu_{\text{C=O}} = 1830 \text{ cm}^{-1}$) becomes significantly more electrophilic than the ketone ($\nu_{\text{C=O}} = 1773 \text{ cm}^{-1}$) and should become the more reactive site in this molecule. This change is further reflected by the C=O bond lengths in the neutral and N-protonated amides (amide/ketone C=O bond lengths of 1.227/1.220 Å in the neutral amide and

1.197/1.211 Å in the N-protonated amide). From an experimental perspective, this finding suggests that chemo-selective transformations of N-activated amides in the presence of carbonyl functionalities should be feasible. Notably, N-protonation of amides containing the [4.3.1] ring system is facile under standard laboratory conditions.^{10a,34a,b}

In summary, the calculated infrared carbonyl stretching frequencies have been found to be in good agreement with the classical amide bond resonance model: an increase in $\nu_{\text{C=O}}$ has been observed with increasing pyramidalization at nitrogen, which reflects the extent of the $n_{\text{N}} \rightarrow \pi^*_{\text{C=O}}$ conjugation. We have demonstrated that infrared spectroscopy gives very accurate predictions of the amide bond distortion parameters, including those of N- and O-protonated amides. Thus, a simple infrared measurement in conjunction with the τ and χ_{N} correlations can be used to provide an estimate of the amide bond distortion in nonplanar amides.

CONCLUSIONS

Changes that occur during rotation around the N–C(O) axis in one-carbon-bridged twisted amides have been studied using ab initio molecular orbital methods. The calculated structures and energies of more than 20 distinct scaffolds ranging from [2.2.1] to [6.3.1] ring systems validate the use of small- and medium-sized one-carbon-bridged twisted amides as models for a systematic study of geometric changes that occur during the rotation of amide bonds. The selected set of bridged amides covers the whole spectrum of amide bond distortion geometries. In the 12 parent scaffolds, the twist angle changes from essentially planar to fully perpendicular ($\tau = 11.32\text{--}90.0^\circ$), while pyramidalization at nitrogen varies from essentially sp^2 -hybridized to fully sp^3 -hybridized nitrogen ($\chi_{\text{N}} = 5.99\text{--}71.44^\circ$). In contrast, the carbonyl carbon remains essentially planar in the series ($\chi_{\text{C}} = 0.0\text{--}15.42^\circ$). The length of the N–C(O) bond varies between 1.474 and 1.365 Å, while the length of the C=O bond is between 1.201 and 1.228 Å. Thus, an increase in the amide bond distortion results in a significant lengthening of the N–C(O) bond, while the C=O bond remains relatively unchanged. This provides strong support for the classical resonance model. Determination of the structural parameters and energies of the more advanced ring scaffolds provides significant insight into previous experimental results and highlights the importance of conformational constraint to achieve gradual levels of distortion of amide bonds within the same ring system of bridged lactams.

The calculated resonance energies indicate that the parent one-carbon-bridged lactams can be classified into three groups: (i) lactams in which the resonance energy virtually disappears or is very low (1.4–5.1 kcal/mol), (ii) lactams in which the resonance energy is calculated to be moderate (9.4–10.7 kcal/mol), and (iii) lactams in which the resonance energy corresponds to that of a typical amide bond (16.0–18.0 kcal/mol). N-Protonation results in a significant lengthening of the N–C(O) bond (average lengthening of 0.169 Å), while the C=O bond undergoes moderate shortening (average shortening of 0.031 Å). O-Protonation results in a considerable lengthening of the C=O bond (average lengthening of 0.090 Å), while the N–C(O) bond shortens to a similar extent (average shortening of 0.087 Å). In eight of the O-protonated lactams, the C=O bond is longer than the N–C(O) bond, which provides a compelling argument for the classical resonance theory.

Calculation of proton affinities reveals that the studied lactams can be divided into two groups: (i) amides that favor protonation at nitrogen ($\Delta\text{PA} = 4.3\text{--}37.5$ kcal/mol), and (ii) amides that favor O-protonation ($\Delta\text{PA} = -4.5$ to -12.8 kcal/mol). An exception is the [5.4.1] ring system, which is calculated to favor N-protonation by only 0.9 kcal/mol. This ring system is predicted to undergo both O- and N-protonation close to equilibrium. Notably, an excellent linear correlation between ΔPA and the sum of the twist angle and pyramidalization at nitrogen has been found. This provides a compelling answer to the long-standing question of structural factors governing the N- versus O-protonation switch in nonplanar lactams. The $\Sigma_{(\tau+\chi_{\text{N}})}$ value of around $50\text{--}60^\circ$ appears to be close to a barrier between N- and O-protonation of amides. This is much lower than the distortion that would correspond to a fully perpendicular amide bond ($\Sigma_{(\tau+\chi_{\text{N}})} = 150.0^\circ$), which has been proposed to be required for efficient N-protonation.

The calculated core ionization energies, atomic charges, frontier molecular orbitals, and infrared frequencies provide further insight into the electronic changes in amide bonds that occur during rotation along the N–C(O) axis. The energies of the frontier molecular orbitals can be correlated with ΔPA , and this can be used as a valuable predictor of the protonation sites of the bridged lactams. Furthermore, the infrared carbonyl stretching frequency ($\nu_{\text{C=O}}$) serves as an accurate predictor of the amide bond distortion parameters, including those of N-protonated amides.

Notably, the presented arguments strongly support the classical amide bond resonance model in predicting the properties of nonplanar amide linkages. More specifically, the changes in bond lengths, pyramidalization at nitrogen, N- and O-protonation, charges, core ionization energies, and infrared carbonyl stretching frequencies that occur upon rotation from planarity to the perpendicular transition state support the classical resonance model. The linear correlation involving the twist angle and pyramidalization at N is further consistent with the classical resonance model. We hope that the understanding of the effects of amide bond rotation provided here will contribute to the rational application of nonplanar amides in medicinal and organic chemistry. For example, a wide range of applications to expand the scope of the intriguing C–N hydrogenolysis reactions of bridged lactams can be readily envisioned. Theoretical investigations of other classes of nonplanar molecules are ongoing, and these results will be reported shortly.

■ ASSOCIATED CONTENT

● Supporting Information

Figures, tables, charts, and text giving the following: (1) Cartesian coordinates and energies with zero-point energy and thermal corrections for all calculated species; (2) detailed description of the computational methods used; (3) extended Tables 5, 6, 7, and 9; (4) extended discussion regarding infrared spectroscopy; (5) extended correlations between structural and energetic parameters discussed in the main text; (6) additional correlations between structural and energetic parameters discussed in the main text; (7) graphical representations of HOMO and LUMO for lactams A–L; (8) graphical representations of optimized geometries of lactams discussed in the main text and reference amides; and (9) full citation of ref 40. The Supporting Information is available free of charge

on the ACS Publications website at DOI: 10.1021/acs.joc.5b00881.

■ AUTHOR INFORMATION

Corresponding Author

*E-mail: michal.szostak@rutgers.edu.

Notes

The authors declare no competing financial interest.

■ ACKNOWLEDGMENTS

We thank the Centre for Networking and Supercomputing (Grant WCSS159), the NIH (Grant GM-49093 to J.A.), and Rutgers University (M.S.) for support.

■ REFERENCES

- (1) A preliminary communication on the computational model to predict protonation sites in bridged lactams has been published. See: Szostak, R.; Aubé, J.; Szostak, M. *Chem. Commun.* **2015**, *51*, 6395.
- (2) (a) *The Amide Linkage: Structural Significance in Chemistry, Biochemistry, and Materials Science*; Greenberg, A.; Breneman, C. M.; Liebman, J. F., Eds.; Wiley: New York, 2000. (b) Pauling, L. *The Nature of the Chemical Bond*; Cornell University Press: Ithaca, NY, 1939.
- (3) For selected examples, see: (a) Kemnitz, C. R.; Loewen, M. J. *J. Am. Chem. Soc.* **2007**, *129*, 2521. (b) Mujika, J. I.; Matxain, J. M.; Eriksson, L. A.; Lopez, X. *Chem. - Eur. J.* **2006**, *12*, 7215. (c) Jean, Y.; Demachy, I.; Lledos, A.; Maseras, F. *J. Mol. Struct.: THEOCHEM* **2003**, *632*, 131. (d) Cho, S. J.; Cui, C.; Lee, J. Y.; Park, J. K.; Suh, S. B.; Park, J.; Kim, B. H.; Kim, K. S. *J. Org. Chem.* **1997**, *62*, 4068. (e) Mucsi, Z.; Tsai, A.; Szori, M.; Chass, G. A.; Viskolcz, B.; Csizmadia, I. G. *J. Phys. Chem. A* **2007**, *111*, 13245. (f) Mucsi, Z.; Chass, G. A.; Viskolcz, B.; Csizmadia, I. G. *J. Phys. Chem. A* **2008**, *112*, 9153. (g) Mucsi, Z.; Chass, G. A.; Csizmadia, I. G. *J. Phys. Chem. B* **2008**, *112*, 7885. (h) Glover, S. A.; Rosser, A. A. *J. Org. Chem.* **2012**, *77*, 5492. (i) Morgan, J.; Greenberg, A.; Liebman, J. F. *Struct. Chem.* **2012**, *23*, 197. (j) Matsubara, T.; Ueta, C. *J. Phys. Chem. A* **2014**, *118*, 8664. (k) Jean, Y.; Demachy, I.; Lledos, A.; Maseras, F. *J. Mol. Struct.: THEOCHEM* **2003**, *632*, 131.
- (4) For selected examples, see: (a) Wang, Q. P.; Bennet, A. J.; Brown, R. S.; Santarsiero, B. D. *J. Am. Chem. Soc.* **1991**, *113*, 5757. (b) Morgan, J.; Greenberg, A. *J. Phys. Org. Chem.* **2012**, *25*, 1422. (c) Otani, Y.; Nagae, O.; Naruse, Y.; Inagaki, S.; Ohno, M.; Yamaguchi, K.; Yamamoto, G.; Uchiyama, M.; Ohwada, T. *J. Am. Chem. Soc.* **2003**, *125*, 15191. (d) Hori, T.; Otani, Y.; Kawahata, M.; Yamaguchi, K.; Ohwada, T. *J. Org. Chem.* **2008**, *73*, 9102. (e) Bednarova, L.; Malon, P.; Bour, P. *Chirality* **2007**, *19*, 775. (f) Yamada, S. *Angew. Chem., Int. Ed. Engl.* **1995**, *34*, 1113. (g) Yamada, S. *J. Org. Chem.* **1996**, *61*, 941. (h) Yamada, S.; Nakamura, M.; Kawachi, I. *Chem. Commun.* **1997**, 885. (i) Morgan, K. M.; Ashline, D. J.; Morgan, J. P.; Greenberg, A. *J. Org. Chem.* **2014**, *79*, 517. (j) Greenberg, A.; Moore, D. T. *J. Mol. Struct.* **1997**, *413–414*, 477. (k) Ly, T.; Krout, M.; Pham, D. K.; Tani, K.; Stoltz, B. M.; Julian, R. R. *J. Am. Chem. Soc.* **2007**, *129*, 1864. For selected synthetic studies, see: (l) Nahm, S.; Weinreb, S. M. *Tetrahedron Lett.* **1981**, *22*, 3815. (m) Balasubramaniam, S.; Aidhen, I. S. *Synthesis* **2008**, *2008*, 3707. (n) Seebach, D. *Angew. Chem., Int. Ed.* **2011**, *50*, 96. (o) Bechara, W. S. J.; Pelletier, G.; Charette, A. B. *Nat. Chem.* **2012**, *4*, 228. (p) Xiao, K. J.; Wang, A. E.; Huang, P. Q. *Angew. Chem., Int. Ed.* **2012**, *51*, 8314. (q) Xiao, K. J.; Luo, J. M.; Ye, K. Y.; Wang, Y.; Huang, P. Q. *Angew. Chem., Int. Ed.* **2010**, *49*, 3037. (r) Tebbe, F. N.; Parshall, G. W.; Reddy, G. S. *J. Am. Chem. Soc.* **1978**, *100*, 3611. (s) Petasis, N. A.; Bzowej, E. I. *J. Am. Chem. Soc.* **1990**, *112*, 6392. (t) Chaplinski, V.; de Meijere, A. *Angew. Chem., Int. Ed. Engl.* **1996**, *35*, 413. (u) de Meijere, A.; Kozhushkov, S. I.; Savchenko, A. I. *J. Organomet. Chem.* **2004**, *689*, 2033. (v) Pace, V.; Holzer, W.; Olofsson, B. *Adv. Synth. Catal.* **2014**, *356*, 3686.
- (5) Wiberg, K. B. Origin of the Amide Rotational Barrier. In *The Amide Linkage: Structural Significance in Chemistry, Biochemistry, and*

Materials Science; Greenberg, A., Breneman, C. M., Liebman, J. F., Eds.; Wiley: New York, 2000.

(6) (a) Ramachandran, G. N. *Biopolymers* **1968**, *6*, 1494. (b) MacArthur, M. W.; Thornton, J. M. *J. Mol. Biol.* **1996**, *264*, 1180. (c) Chalupsky, J.; Vondrasek, J.; Spirko, V. *J. Phys. Chem. A* **2008**, *112*, 693. (d) Shin, S. B. Y.; Yoo, B.; Todaro, L. J.; Kirshenbaum, K. *J. Am. Chem. Soc.* **2007**, *129*, 3218. (e) Poteau, R.; Trinquier, G. *J. Am. Chem. Soc.* **2005**, *127*, 13875.

(7) Wiberg, K. B.; Laidig, K. E. *J. Am. Chem. Soc.* **1987**, *109*, 5935.

(8) Greenberg, A. The Amide Linkage as a Ligand—Its Properties and the Role of Distortion. In *The Amide Linkage: Structural Significance in Chemistry, Biochemistry, and Materials Science*; Greenberg, A., Breneman, C. M., Liebman, J. F., Eds.; Wiley: New York, 2000.

(9) (a) Brown, R. S.; Bennet, A. J.; Slebocka-Tilk, H. *Acc. Chem. Res.* **1992**, *25*, 481. (b) Radzicka, A.; Wolfenden, R. *J. Am. Chem. Soc.* **1996**, *118*, 6105. (c) Kahne, D.; Still, W. C. *J. Am. Chem. Soc.* **1988**, *110*, 7529.

(10) For reviews, see: (a) Szostak, M.; Aubé, J. *Chem. Rev.* **2013**, *113*, 5701. (b) Szostak, M.; Aubé, J. *Org. Biomol. Chem.* **2011**, *9*, 27. (c) Hall, H. K., Jr.; El-Shekeil, A. *Chem. Rev.* **1983**, *83*, 549. (d) Yamada, S. *Rev. Heteroat. Chem.* **1999**, *19*, 203. (e) Yamada, S. Sterically Hindered Twisted Amides. In *The Amide Linkage: Structural Significance in Chemistry, Biochemistry, and Materials Science*; Greenberg, A., Breneman, C. M., Liebman, J. F., Eds.; Wiley: New York, 2000. (f) Glover, S. A. *Adv. Phys. Org. Chem.* **2007**, *42*, 35.

(11) Lease, T. G.; Shea, K. J. A Compilation and Analysis of Structural Data of Distorted Bridgehead Olefins and Amides. In *Advances in Theoretically Interesting Molecules*; JAI Press: Greenwich, CT, 1992; Vol. 2.

(12) (a) Clayden, J.; Moran, W. J. *Angew. Chem., Int. Ed.* **2006**, *45*, 7118. (b) Clayden, J. *Nature* **2012**, *481*, 274. (c) Aubé, J. *Angew. Chem., Int. Ed.* **2012**, *51*, 3063.

(13) For amide bond proteolysis, see: (a) Somayaji, V.; Brown, R. S. *J. Org. Chem.* **1986**, *51*, 2676. (b) Williams, A. *J. Am. Chem. Soc.* **1976**, *98*, 5645. (c) Perrin, C. L. *Acc. Chem. Res.* **1989**, *22*, 268. For cis–trans isomerization, see: (d) Liu, J.; Albers, M. W.; Chen, C. M.; Schreiber, S. L.; Walsh, C. T. *Proc. Natl. Acad. Sci. U. S. A.* **1990**, *87*, 2304. (e) Fischer, G. *Chem. Soc. Rev.* **2000**, *29*, 119. (f) Fischer, G.; Schmid, F. X. Peptidyl–Prolyl Cis/Trans Isomerases. In *Molecular Chaperones and Folding Catalysts: Regulation, Cellular Functions and Mechanisms*; Bakau, B., Ed.; CRC Press: Boca Raton, FL, 1999. For protein splicing, see: (g) Poland, B. W.; Xu, M. Q.; Quioco, F. A. *J. Biol. Chem.* **2000**, *275*, 16408. (h) Romanelli, A.; Shekhtman, A.; Cowburn, D.; Muir, T. W. *Proc. Natl. Acad. Sci. U. S. A.* **2004**, *101*, 6397. (i) Shemella, P.; Pereira, B.; Zhang, Y. M.; van Roey, P.; Belfort, G.; Garde, S.; Nayak, S. K. *Biophys. J.* **2007**, *92*, 847. (j) Johansson, D. G. A.; Wallin, G.; Sandberg, A.; Macao, B.; Aqvist, J.; Hard, T. *J. Am. Chem. Soc.* **2009**, *131*, 9475. For β -lactam antibiotics, see: (k) Georg, G. I. *The Organic Chemistry of β -Lactams*; Wiley-VCH: Weinheim, Germany, 1992. (l) Bose, A. K.; Manhas, M. S.; Banik, B. K.; Srirajan, V. β -Lactams: Cyclic Amides of Distinction. In *The Amide Linkage: Structural Significance in Chemistry, Biochemistry, and Materials Science*; Greenberg, A., Breneman, C. M., Liebman, J. F., Eds.; Wiley: New York, 2000. For conformational preferences of peptides, see: (m) Hosoya, M.; Otani, Y.; Kawahata, M.; Yamaguchi, K.; Ohwada, T. *J. Am. Chem. Soc.* **2010**, *132*, 14780. (n) Stringer, J. R.; Crapster, J. A.; Guzei, I. A.; Blackwell, H. E. *J. Org. Chem.* **2010**, *75*, 6068. (o) Wang, S.; Otani, Y.; Liu, X.; Kawahata, M.; Yamaguchi, K.; Ohwada, T. *J. Org. Chem.* **2014**, *79*, 5287. For chemical space, see: (p) Burke, M. D.; Schreiber, S. L. *Angew. Chem., Int. Ed.* **2004**, *43*, 46. (q) Galloway, W. R. J. D.; Isidro-Llobet, A.; Spring, D. R. *Nat. Commun.* **2010**, *1*, No. 80. (r) Brown, L. E.; Cheng, K. C.-C.; Wei, W. G.; Yuan, P.; Dai, P.; Trilles, R.; Ni, F.; Yuan, J.; MacArthur, R.; Guha, R.; Johnson, R. L.; Su, X. Z.; Dominguez, M. M.; Snyder, J. K.; Beeler, A. B.; Schaus, S. E.; Inglese, J.; Porco, J. A., Jr. *Proc. Natl. Acad. Sci. U. S. A.* **2011**, *108*, 6775. (s) Virshup, A. M.; Contreras-García, J.; Wipf, P.; Yang, W.; Beratan, D. N. *J. Am. Chem. Soc.* **2013**, *135*, 7296.

(14) (a) Wiberg, K. B. *Acc. Chem. Res.* **1999**, *32*, 922. (b) Wiberg, K. B.; Breneman, C. M. *J. Am. Chem. Soc.* **1992**, *114*, 831. (c) Perrin, C. L. *J. Am. Chem. Soc.* **1991**, *113*, 2865. (d) Wiberg, K. B.; Rablen, P. R. *J. Am. Chem. Soc.* **1993**, *115*, 9234. (e) Laidig, K. E.; Cameron, L. M. *J. Am. Chem. Soc.* **1996**, *118*, 1737. (f) Wiberg, K. B.; Rablen, P. R. *J. Am. Chem. Soc.* **1993**, *115*, 9234. (g) Bennet, A. J.; Somayaji, V.; Brown, R. S.; Santarsiero, B. D. *J. Am. Chem. Soc.* **1991**, *113*, 7563. It is worth noting that according to the Wiberg–Bader theory of atoms in molecules (AIM), the stability of the planar amide bond relative to the orthogonal amide bond results from a hybridization change at nitrogen. For a detailed discussion see refs 14a,g and 3a.

(15) Lukeš, R. *Collect. Czech. Chem. Commun.* **1938**, *10*, 148.

(16) (a) Wasserman, H. H. *Nature* **2006**, *441*, 699. (b) Woodward, R. B.; Neuberger, A.; Trenner, N. R. *The Chemistry of Penicillin*. In *The Chemistry of Penicillin*; Clarke, H. T., Johnson, J. R., Robinson, R., Eds.; Princeton University Press: Princeton, NJ, 1949.

(17) (a) Yakhontov, L. N.; Rubtsov, M. V. *J. Gen. Chem. USSR* **1957**, *27*, 83. (b) Levkoeva, E. I.; Nikitskaya, E. S.; Yakhontov, L. N. *Dokl. Akad. Nauk* **1970**, *192*, 342. (c) Levkoeva, E. I.; Nikitskaya, E. S.; Yakhontov, L. N. *Khim. Geterotsikl. Soedin.* **1971**, 378.

(18) (a) Pracejus, H. *Chem. Ber.* **1959**, *92*, 988. (b) Pracejus, H.; Kehlen, M.; Kehlen, H.; Matschiner, H. *Tetrahedron* **1965**, *21*, 2257. (c) Pracejus, H. *Chem. Ber.* **1965**, *98*, 2897.

(19) Tani, K.; Stoltz, B. M. *Nature* **2006**, *441*, 731.

(20) (a) Bennet, A. J.; Wang, Q. P.; Slebocka-Tilk, H.; Somayaji, V.; Brown, R. S.; Santarsiero, B. D. *J. Am. Chem. Soc.* **1990**, *112*, 6383. (b) Wang, Q. P.; Bennet, A. J.; Brown, R. S.; Santarsiero, B. D. *Can. J. Chem.* **1990**, *68*, 1732. (c) Blackburn, G. M.; Skaife, C. J.; Kay, I. T. *J. Chem. Res., Synop.* **1980**, 294.

(21) (a) Shea, K. J.; Lease, T. G.; Ziller, J. W. *J. Am. Chem. Soc.* **1990**, *112*, 8627. (b) Lease, T. G.; Shea, K. J. *J. Am. Chem. Soc.* **1993**, *115*, 2248.

(22) (a) Kirby, A. J.; Komarov, I. V.; Wothers, P. D.; Feeder, N. *Angew. Chem., Int. Ed.* **1998**, *37*, 785. (b) Kirby, A. J.; Komarov, I. V.; Feeder, N. *J. Am. Chem. Soc.* **1998**, *120*, 7101. (c) Kirby, A. J.; Komarov, I. V.; Feeder, N. *J. Chem. Soc., Perkin Trans. 2* **2001**, 522. The synthesis of the parent ring system of “Kirby’s amide” has been recently achieved. See: (d) Komarov, I. V.; Yanik, S.; Ishchenko, A. Y.; Davies, J. E.; Goodman, J. M.; Kirby, A. J. *J. Am. Chem. Soc.* **2015**, *137*, 926.

(23) Bashore, C. G.; Samardjiev, I. J.; Bordner, J.; Coe, J. W. *J. Am. Chem. Soc.* **2003**, *125*, 3268.

(24) (a) Greenberg, A.; Venanzi, C. A. *J. Am. Chem. Soc.* **1993**, *115*, 6951. (b) Greenberg, A.; Moore, D. T.; DuBois, T. D. *J. Am. Chem. Soc.* **1996**, *118*, 8658.

(25) (a) Lopez, X.; Mujika, J. I.; Blackburn, G. M.; Karplus, M. *J. Phys. Chem. A* **2003**, *107*, 2304. (b) Mujika, J. I.; Mercero, J. M.; Lopez, X. *J. Phys. Chem. A* **2003**, *107*, 6099. (c) Mujika, J. I.; Mercero, J. M.; Lopez, X. *J. Am. Chem. Soc.* **2005**, *127*, 4445. (d) Mujika, J. I.; Formoso, E.; Mercero, J. M.; Lopez, X. *J. Phys. Chem. B* **2006**, *110*, 15000. (e) Wang, B.; Cao, Z. *Chem. - Eur. J.* **2011**, *17*, 11919.

(26) Morgan, K. M.; Rawlins, M. L.; Montgomery, M. N. *J. Phys. Org. Chem.* **2005**, *18*, 310.

(27) For representative examples of larger ring systems of twisted amides, see: (a) Aszodi, J.; Rowlands, D. A.; Mauvais, P.; Collette, P.; Bonnefoy, A.; Lampilas, M. *Bioorg. Med. Chem. Lett.* **2004**, *14*, 2489. (b) Buchanan, G. L.; Kitson, D. H.; Mallinson, P. R.; Sim, G. A.; White, D. N. J.; Cox, P. J. *J. Chem. Soc., Perkin Trans. 2* **1983**, 1709. (c) Grigg, R.; Sridharan, V.; Stevenson, P.; Worakun, T. *J. Chem. Soc., Chem. Commun.* **1986**, 1697. (d) Ribelin, T. P.; Judd, A. S.; Akritopoulou-Zanze, I.; Henry, R. F.; Cross, J. L.; Whittern, D. N.; Djuric, S. W. *Org. Lett.* **2007**, *9*, 5119. (e) Dexter, D. D.; van der Veen, J. M. *J. Chem. Soc., Perkin Trans. 1* **1978**, 185. (f) Wang, A. H. J.; Paul, I. C.; Talaty, E. R.; Dupuy, A. E. *J. Chem. Soc., Chem. Commun.* **1972**, 43. (g) Kirby, A. J.; Komarov, I. V.; Kowski, K.; Rademacher, P. *J. Chem. Soc., Perkin Trans. 2* **1999**, 1313. For the X-ray structure of N-methyl-2-piperidone, see: (h) Moragues-Bartolome, A. M.; Jones, W.; Cruz-Cabeza, A. J. *CrystEngComm* **2012**, *14*, 2552.

(28) Yao, L.; Aubé, J. *J. Am. Chem. Soc.* **2007**, *129*, 2766.

- (29) (a) Ma, J. C.; Dougherty, D. A. *Chem. Rev.* **1997**, *97*, 1303–1324. (b) Meyer, E. A.; Castellano, R. K.; Diederich, F. *Angew. Chem., Int. Ed.* **2003**, *42*, 1210–1250. (c) Yamada, S. *Org. Biomol. Chem.* **2007**, *5*, 2903–2912. (d) Smith, D. M.; Woerpel, K. A. *Org. Biomol. Chem.* **2006**, *4*, 1195–1201.
- (30) Milligan, G. L.; Mossman, C. J.; Aubé, J. *J. Am. Chem. Soc.* **1995**, *117*, 10449.
- (31) For methods of synthesis of one-carbon-bridged amides, see: (a) Szostak, M.; Aubé, J. *Org. Lett.* **2009**, *11*, 3878. (b) Szostak, M.; Yao, L.; Aubé, J. *Org. Lett.* **2009**, *11*, 4386. (c) Szostak, M.; Yao, L.; Aubé, J. *J. Org. Chem.* **2010**, *75*, 1235. (d) Macleod, F.; Lang, S.; Murphy, J. A. *Synlett* **2010**, 529. (e) Szostak, M. Ph.D. Thesis, University of Kansas, Lawrence, KS, 2009. (f) Williams, R. M.; Lee, B. H.; Miller, M. M.; Anderson, O. P. *J. Am. Chem. Soc.* **1989**, *111*, 1073. (g) Fuchs, J. R.; Funk, R. L. *J. Am. Chem. Soc.* **2004**, *126*, 5068. (h) Nazarenko, K. G.; Shtil, N. A.; Buth, S. A.; Chernega, A. N.; Lozinskii, M. O.; Tolmachev, A. A. *Tetrahedron* **2008**, *64*, 4478. (i) Schill, G.; Priester, C. U.; Windhövel, U. F.; Fritz, H. *Helv. Chim. Acta* **1986**, *69*, 438. (j) Schill, G.; Löwer, H.; Priester, C. U.; Windhövel, U. F.; Fritz, H. *Tetrahedron* **1987**, *43*, 3729. (k) Schill, G.; Priester, C. U.; Windhövel, U. F.; Fritz, H. *Tetrahedron* **1990**, *46*, 1221. (l) Ban, Y.; Yoshida, K.; Goto, J.; Oishi, T. *J. Am. Chem. Soc.* **1981**, *103*, 6990. (m) Bremner, J. B.; Eschler, B. M.; Skelton, B. W.; White, A. H. *Aust. J. Chem.* **1994**, *47*, 1935. (n) Schumann, D.; Geirsson, J.; Naumann, A. *Chem. Ber.* **1985**, *118*, 1927. (o) Bahadur, G. A.; Bailey, A. S.; Scott, P. W.; Vandrevala, M. H. *J. Chem. Soc., Perkin Trans. 1* **1980**, 2870.
- (32) Winkler, F. K.; Dunitz, J. D. *J. Mol. Biol.* **1971**, *59*, 169. The Winkler–Dunitz distortion parameters τ , χ_N , and χ_C describe the magnitude of rotation around the N–C(O) bond (i.e., the twist angle), the pyramidalization at nitrogen, and pyramidalization at carbon, respectively. τ is 0° for planar amide bonds and 90° for fully orthogonal bonds; χ_N and χ_C are 0° for planar bonds and 60° for fully pyramidalized amide bonds.
- (33) Lei, Y.; Wroblewski, A. D.; Golden, J. E.; Powell, D. R.; Aubé, J. *J. Am. Chem. Soc.* **2005**, *127*, 4552.
- (34) (a) Szostak, M.; Yao, L.; Day, V. W.; Powell, D. R.; Aubé, J. *J. Am. Chem. Soc.* **2010**, *132*, 8836. (b) Sliter, B.; Morgan, J.; Greenberg, A. *J. Org. Chem.* **2011**, *76*, 2770. For examples of electrophilic reactivity of twisted amides, see: (c) Szostak, M.; Yao, L.; Aubé, J. *J. Am. Chem. Soc.* **2010**, *132*, 2078. (d) Szostak, M.; Aubé, J. *J. Am. Chem. Soc.* **2009**, *131*, 13246. (e) Szostak, M.; Aubé, J. *Chem. Commun.* **2009**, 7122.
- (35) Szostak, M.; Yao, L.; Aubé, J. *J. Org. Chem.* **2009**, *74*, 1869.
- (36) For representative examples of other classes of twisted amides, see: Anomeric amides: (a) Glover, S. A. *Tetrahedron* **1998**, *54*, 7229. (b) Glover, S. A.; Mo, G.; Rauk, A.; Tucker, D. J.; Turner, P. J. *Chem. Soc., Perkin Trans. 2* **1999**, 2053. Sterically-hindered amides: (c) Yamada, S. *Angew. Chem., Int. Ed. Engl.* **1993**, *32*, 1083. For an elegant example of sterically-hindered amides activated by a proton-switch mechanism, see: (d) Hutchby, M.; Houlden, C. E.; Haddow, M. F.; Tyler, S. N.; Lloyd-Jones, G. C.; Booker-Milburn, K. I. *Angew. Chem., Int. Ed.* **2012**, *51*, 548.
- (37) Morgan, J.; Greenberg, A. *J. Chem. Thermodyn.* **2014**, *73*, 206. This elegant article reports selected structural parameters of various bridged lactams using a rapid density functional theory method (B3LYP/6-31G*).
- (38) (a) Szostak, M.; Spain, M.; Procter, D. J. *Angew. Chem., Int. Ed.* **2013**, *52*, 7237. For a lead review of lanthanide(II) reagents, see: (b) Szostak, M.; Fazakerley, N. J.; Parmar, D.; Procter, D. J. *Chem. Rev.* **2014**, *114*, 5959.
- (39) Hayes, C. J.; Simpkins, N. S.; Kirk, D. T.; Mitchell, L.; Baudoux, J.; Blake, A. J.; Wilson, C. *J. Am. Chem. Soc.* **2009**, *131*, 8196.
- (40) Frisch, M. J.; et al. *Gaussian 09*, revision D.01; Gaussian, Inc.: Wallingford, CT, 2009.
- (41) (a) Maier, W. F.; Schleyer, P. V. *J. Am. Chem. Soc.* **1981**, *103*, 1891. (b) Warner, P. M. *Chem. Rev.* **1989**, *89*, 1067.
- (42) (a) Sparks, S. M.; Vargas, J. D.; Shea, K. J. *Org. Lett.* **2000**, *2*, 1473. (b) Sparks, S. M.; Chow, C. P.; Zhu, L.; Shea, K. J. *J. Org. Chem.* **2004**, *69*, 3025. (c) Chow, C. P.; Shea, K. J.; Sparks, S. M. *Org. Lett.* **2002**, *4*, 2637. (d) Molina, C. L.; Chow, C. P.; Shea, K. J. *J. Org. Chem.* **2007**, *72*, 6816.
- (43) For lead references on using bridged lactams in medicinal chemistry, see: (a) Reference 27a. (b) Mangion, I. K.; Ruck, R. T.; Rivera, N.; Huffman, M. A.; Shevlin, M. *Org. Lett.* **2011**, *13*, 5480. (c) Brouillette, W. J.; Grunewald, G. L.; Brown, G. B.; DeLorey, T. M.; Akhtar, M. S.; Liang, G. *J. Med. Chem.* **1989**, *32*, 1577. (d) Brouillette, W. J.; Jestkov, V. P.; Brown, M. L.; Akhtar, M. S.; DeLorey, T. M.; Brown, G. B. *J. Med. Chem.* **1994**, *37*, 3289. (e) Grimm, J. B.; Stables, J. P.; Brown, M. L. *Bioorg. Med. Chem.* **2003**, *11*, 4133. (f) Murakami, M.; Aoki, T.; Nagata, W. *Synlett* **1990**, 1990, 684. (g) Buynak, J. D.; Rao, A. S.; Adam, G.; Nidamarthy, S. D.; Zhang, H. *J. Am. Chem. Soc.* **1998**, *120*, 6846. (h) Hans, R. H.; Wiid, I. J. F.; van Helden, P. D.; Wan, B.; Franzblau, S. G.; Gut, J.; Rosenthal, P. J.; Chibale, K. *Bioorg. Med. Chem. Lett.* **2011**, *21*, 2055.
- (44) Werstki, N. H.; Brown, R. S.; Wang, Q. *Can. J. Chem.* **1996**, *74*, 524.
- (45) Cox, C.; Wack, H.; Lectka, T. *Angew. Chem., Int. Ed.* **1999**, *38*, 798.
- (46) (a) For a discussion of the RE of O-protonated amides see ref 24a. For other relevant references, see: (b) Olah, G. A.; White, A. M.; O'Brien, D. H. *Chem. Rev.* **1970**, *70*, 561. (c) Klumpp, D. A.; Rendsy; Zhang, Y.; Gomez, A.; McElrea, A. *Org. Lett.* **2004**, *6*, 1789. (d) Birchall, T.; Gillespie, R. J. *Can. J. Chem.* **1963**, *41*, 2642. (e) Howard, A. E.; Kollman, P. A. *J. Am. Chem. Soc.* **1988**, *110*, 7195. (f) Lias, S. G.; Bartmess, J. E.; Liebman, J. F.; Holmes, J. L.; Levin, R. D.; Mallard, W. G. *J. Phys. Chem. Ref. Data* **1988**, *17* (Suppl. 1). (g) Benedetti, E.; Di Blasio, B.; Baine, P. *J. Chem. Soc., Perkin Trans. 2* **1980**, 500.
- (47) Cox, C.; Lectka, T. *Acc. Chem. Res.* **2000**, *33*, 849.
- (48) (a) Deslongchamps, P. *Stereoelectronic Effects in Organic Chemistry*; Pergamon Press: Oxford, U.K., 1983. (b) Adler, M.; Adler, S.; Boche, G. *J. Phys. Org. Chem.* **2005**, *18*, 193. (c) Evans, D. A.; Borg, G.; Scheidt, K. A. *Angew. Chem., Int. Ed.* **2002**, *41*, 3188.
- (49) Nørskov-Lauritsen, L.; Bürgi, H. B.; Hofmann, P.; Schmidt, H. R. *Helv. Chim. Acta* **1985**, *68*, 76.
- (50) Only a few examples of N-alkylated amides have been reported to date,^{17b,18,34a,44} and none has been characterized by X-ray crystallography. N-Methylation of the tricyclic one-carbon-bridged amide **W**, [4.3.1] has been previously reported.^{34a} We determined that this amide favors N-methylation over O-methylation by 22.4 kcal/mol, which can be compared with a value of 12.7 kcal/mol for N-protonation vs O-protonation (corrected values, MP2/6-311++G(d,p)). The difference likely results from steric interactions of the O-methyl group with the ring scaffold. The N-methylated amide is characterized by the following distortion parameters: $\tau = 68.64^\circ$; $\chi_N = 55.80^\circ$; $\chi_C = 3.00^\circ$; N–C(O) = 1.567 Å; C=O = 1.194 Å, N–Me = 1.502 Å. These can be compared with the values for the N-protonated amide ($\tau = 72.41^\circ$; $\chi_N = 47.83^\circ$; $\chi_C = 1.72^\circ$; N–C(O) = 1.550 Å; C=O = 1.195 Å) and the O-methylated amide ($\tau = 48.65^\circ$; $\chi_N = 28.54^\circ$; $\chi_C = 17.48^\circ$; N–C(O) = 1.323 Å; C=O = 1.306 Å, O–Me = 1.453 Å). Overall, these data indicate that the synthesis of N-alkylated amides should be facile on steric grounds, and the preparation of a wide range of analogues should be feasible.
- (51) (a) Greenberg, A.; Thomas, T. D.; Bevilacqua, C. R.; Coville, M.; Ji, D.; Tsai, J. C.; Wu, G. *J. Org. Chem.* **1992**, *57*, 7093. (b) Hüfner, S. *Photoelectron Spectroscopy: Principles and Applications*; Springer: Berlin, 2003. (c) Brundle, C. R.; Baker, A. D. *Electron Spectroscopy: Theory, Techniques and Applications*; Academic Press: London, 1978. (d) Koopmans, T. *Physica* **1934**, *1*, 104.
- (52) (a) Reed, A. E.; Weinstock, R. B.; Weinhold, F. *J. Chem. Phys.* **1985**, *83*, 735. (b) Sigfridsson, E.; Ryde, U. *J. Comput. Chem.* **1998**, *19*, 377. (c) Martin, F.; Zipse, H. *J. Comput. Chem.* **2005**, *26*, 97. (d) Wiberg, K. B.; Rablen, P. R. *J. Comput. Chem.* **1993**, *14*, 1504.
- (53) (a) Treschanke, L.; Rademacher, P. *J. Mol. Struct.: THEOCHEM* **1985**, *122*, 35. (b) Treschanke, L.; Rademacher, P. *J. Mol. Struct.: THEOCHEM* **1985**, *122*, 47. (c) Woydt, M.; Rademacher, P.; Kaupp, G.; Sauerland, O. *J. Mol. Struct.* **1989**, *192*, 141. (d) Reference 27g.

(e) Werstiuk, N. H.; Muchall, H. M.; Roy, C. D.; Ma, J.; Brown, R. S. *Can. J. Chem.* **1998**, *76*, 672.

(54) Aue, D. H.; Webb, H. M.; Bowers, M. T. *J. Am. Chem. Soc.* **1975**, *97*, 4136.

(55) (a) Stuart, B. H. *Infrared Spectroscopy: Fundamentals and Applications*; Wiley: Chichester, U.K., 2004. (b) Silverstein, R. M.; Bassler, G. C.; Morrill, T. C. *Spectroscopic Identification of Organic Compounds*; Wiley: New York, 1991.

(56) Ledbetter, J. W., Jr. *J. Phys. Chem.* **1977**, *81*, 54.